

THESIS FOR THE DEGREE OF LICENTIATE OF ENGINEERING

Three dimensional mathematical modelling of pronuclei migration for the mouse

Sofia Tapani

CHALMERS



GÖTEBORGS UNIVERSITET

Department of Mathematical Sciences
Division of Mathematical Statistics
Chalmers University of Technology and University of Gothenburg
Göteborg, Sweden 2009

Three dimensional mathematical modelling of pronuclei migration
for the mouse

Sofia Tapani

NO 2009:36

ISSN 1652-9715

©Sofia Tapani, 2009

Department of Mathematical Sciences

Division of Mathematical Statistics

Chalmers University of Technology and University of Gothenburg

SE-412 96 Göteborg

Sweden

Telephone +46 (0)31 772 1000

Typeset with L^AT_EX.

Printed in Göteborg, Sweden 2009

Three dimensional mathematical modelling of pronuclei migration for the mouse

Sofia Tapani

Department of Mathematical Sciences
Division of Mathematical Statistics
Chalmers University of Technology and University of Gothenburg

Abstract

The main question addressed in this thesis is what happens between the moment when the sperm enters the egg and the fusion of the male and the female pronuclei. Orientation of the apposing pronuclei most likely plays a decisive role in the polarity of the developing embryo. The migration and the dependence between the pronuclei have been investigated through three different measures of correlation. It was concluded that a measure based on the projection of the movement onto the axis between the pronuclei's centres was preferred. Two mathematical models that describe the pronuclei dynamics have been constructed in the form of stochastic differential equations. The models concern pronuclei migration from the time of the sperm entry to the fusion and spatial orientation of this fusion. First, a basic model was created. This was then developed into a refined model. The methodology consists of using stacks of confocal microscopy time-lapse images of the pronuclei migration together with statistical methods to identify realistic parameters in the models. Given different angles between the sperm entry and the position of the second polar body, the final models are then used to produce distributions of orientations of the meeting positions between the pronuclei. However, the main result is the suggested models themselves which describe the main features of the migration. The basic fitted model is based on two forces of attraction. Migration is directed towards the centre but also towards the other pronucleus. Parameter values corresponding to the size of these forces are estimated from data of both eggs treated with a microtubule inhibitor and untreated eggs. The refined model is also based on centring and attraction to the other pronucleus, but the centring is modelled into two mechanisms of pushing and pulling of the microtubule exerted forces. Simulated distributions from the models could for instance be used as initial value distributions for future models of egg cleavage.

Keywords: fertilisation process, pronucleus, dynamical simulation, SDE, correlation, CUSUM, microtubule, confocal microscopy

Acknowledgments

I would like to thank my advisor Torbjörn Lundh and my co-advisor Aila Särkkä for their great support. I also would like to thank my co-authors, in addition to my advisor, Jun Udagawa for his great effort in performing the tedious measurements on the confocal data, Berenika Plusa for producing the data material and teaching me how to distinguish between a pronucleus and cytoplasm. Finally, thanks to Magdalena Zernicka-Goetz for welcoming me in her lab and for her invaluable time and comments. Bernhard Strauss, thank you for helping out with discussions and references on microtubule dynamics. I would also like to take the opportunity to thank everyone at Magdalena's lab at the Wellcome trust/Gurdon institute in Cambridge for being so friendly and eager to share their research.

I am very grateful to the administrative personnel and technicians at Mathematical Sciences. Thank you, for always having time for small and big questions.

Thank you friends, both in-water and out-of-water. You are all important. Without you, this thesis might have been finished a lot faster but it would definitely not have been the same and not as much fun. Thanks for helping me live life to the fullest.

The final thanks go to my family and Per for their love and for never stopping to believe in what I can do. Please continue to push me further.

Contents

1	Introduction	1
1.1	Background	1
1.2	The biology of the unfertilised egg	3
1.2.1	Production of reproductive cells	3
1.2.2	Oogenesis and spermatogenesis	3
1.2.3	The fertilisation process	4
2	Data material	7
3	Initial data exploration	13
3.1	Axis-wise correlation	15
3.2	Spherical correlation coefficient	16
3.3	A projection measure	20
3.4	Estimation of phase change by the CUSUM method	22
4	Modelling the pronuclei migration	27
4.1	Microtubules and the migrating pronuclei	28
4.1.1	Dynamical mechanics of the migration	28
4.1.2	Three available biological models for positioning	30

4.2	Mathematical modelling of the pronuclei migration	31
4.2.1	The basic model	32
4.2.2	A refined model	35
4.2.3	Dissecting the noise	36
4.2.4	The complete models	37
5	Parameter estimation	39
5.1	Results for the basic model	40
5.2	Results for the refined model	41
6	Simulation study	43
7	Discussion	49
	Bibliography	52
	Appendix	57

Chapter 1

Introduction

Developmental biology is the biology of the first events the living organism experience. As the microscopy techniques improve and the amount of data increases there is need for better and more effective analysis methods. Mathematical modelling of the microtubule dynamics is now an important interdisciplinary area between mathematics, mathematical statistics, physics and biology. In this chapter we will start with the background of our problem setting and then continue with giving a short summary of the biology behind the fertilisation process for the mouse egg.

1.1 Background

As most mammalian eggs, the mouse egg is a highly regulative system. In being so, it is still an open question when the future fates of the cells are fixed, (Davies and Gardner, 2002), (Davies and Gardner, 2003), (Gardner, 2003), (Hiiragi and Solter, 2004), (Motosugi et al., 2005), (Plusa et al., 2005), (Zernicka-Goetz, 2005), (Zernicka-Goetz, 2006). Currently there exist different viewpoints of how to define total randomness and pattern bias in the egg. The battle is between completely spatial randomness and rigidity and determinative behaviour. Our aim is to show that these two possible explanations do not exclude each other but can both simultaneously affect the cell fates. Cells may have a pattern, or a set of rules, to follow and at the same time be influenced by the stochasticity of the chemical system and the cytoplasmic environment inside the egg.

Cell-fate is flexible, meaning that the development can recover from perturbations (Gilbert, 2006). Previous results indicate that the first cleavage is preferably occurring along the short axis of the egg (Zernicka-Goetz, 2005). The short axis position is in turn related to sperm entry and migration of the pronuclei. The second polar body and the sperm entry point could together make up a coordinate system for the axis formation of the later embryo. Other studies of the mouse's development show deviating results concerning when patterning is initiated in the egg. See for instance (Davies and Gardner, 2002) and (Hiiragi and Solter, 2004). Some of these studies that conclude that the pattern formation starts later in the embryo have however been conducted in 2D. We think it is important to consider this as a 3D problem since ignoring one of the three dimensions may introduce some bias, due to discarding eggs where migration takes place over several confocal planes. Also it is important to use measurement techniques that are the least invasive available to get a true picture of what is actually taking place during the first seconds of the life of the embryo.

One purpose of having a model for the migration is to be able to more easily visualize the fertilisation process to answer questions of biased data. A model of this kind could be used to predict outcomes from for instance the point of sperm entry by simulating different scenarios. It could provide initial conditions to further models of cell division and differentiation. Moreover, values of model parameters can be used to quantify treatment or measurement effects on the egg.

We are using inspiration from developmental biology literature and potential theory to produce a model for the pronuclei migration. In setting up the model, data from confocal time-lapse differential interference contrast (DIC) images of mouse eggs have been used to record the 3D-coordinates of the pronuclei up to the first division of the egg. The work of this thesis has its background in the research of the Magdalena Zernicka-Goetz group at the Gurdon Institute in Cambridge. Her group studies development of spatial patterning and determination of cell fate of the early mouse embryo.

We will in the following section give some background of the biological processes behind the generation of an embryo. In addition to this perhaps simpler description, the beginning of Chapter 4 is devoted to further investigation of the processes that govern the pronuclei dynamics.

1.2 The biology of the unfertilised egg

For the readers who are more mathematically oriented, a short review of the biology of this work will be presented. The production of the reproductive cells of mammals will be handled first. The background to this section is mainly gathered from (Gilbert, 2006) and (Wolpert et al., 1998). Production of the reproductive cells is common for most mammals, such as humans, mice, etc. Reading of this section can be occluded if the reader is familiar with the components involved in the fertilisation process.

1.2.1 Production of reproductive cells

In understanding the difference between fusion of the gametes (the reproductive cells) and ordinary cell division, it is necessary to look into the production of the reproductive cells. Ordinary cell division, where the DNA duplicates itself by undergoing a number of complex processes and the single cell divides into two cells, is called mitosis. During fertilisation the genetic materials from two individuals are fused together. The fusion does not take place in the fertilised egg but it is complete in the two-cell stage. Because the number of chromosomes being constant, the germ cells must divide by reduction division. Division when the chromosome number is reduced is called meiosis. Diploid precursors for the gametes have two copies of each chromosome, one maternal and one paternal. The number of copies is halved during meiosis so that the gametes contain only one copy of each chromosome. Diploid number of the chromosomes will be restored at fertilisation.

1.2.2 Oogenesis and spermatogenesis

Oogenesis is the production of eggs. First, the germ cells that form the eggs divide mitotically a few times and then they enter prophase of the first meiotic division. No further cell multiplication occur after this. Further development of the egg occurs as the female becomes sexually mature. After the ovulation, completion of the first meiotic division takes place and the first polar body is formed. The egg is now blocked at the second metaphase of meiosis until fertilisation starts. After fertilisation, the second polar body will be formed and the division of the genetic material is now complete. At this point, the maternal genetic material concentrated in a pronucleus is present in the egg at the position next to the second polar body. See Figure 1.1.

Spermatogenesis is the production of the sperms. Germ cells that develop into

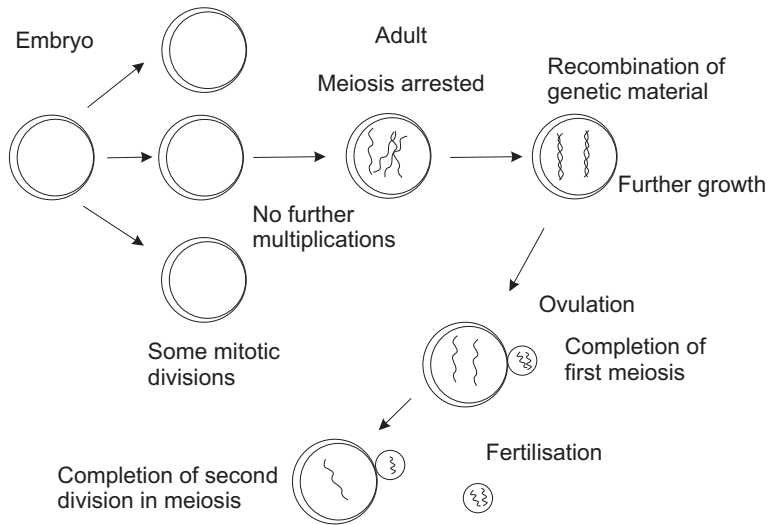


Figure 1.1: Production cycle of the egg cell, during a mammal's life from embryo to adult.

sperm enter the embryonic testis and become arrested in the cell cycle. After birth, the cells start to divide mitotically, forming a population of stem cells. These give off cells that divide meiotically and then differentiate into sperm. This process is depicted in Figure 1.2.

1.2.3 The fertilisation process

Fusion of the sperm and the egg is the start of the development. Its purpose is to transfer genetic material from parents to offspring. At the time when the sperm enters, the egg is arrested in metaphase of its second meiotic division. Formation of the female pronucleus is completed as the sperm enters the egg, see Figure 1.3. Cell membranes of the egg and the sperm fuse and the sperm enters the egg's cytoplasm, where it transforms into the male pronucleus. Still there are some parts of the sperm tail left which in some cases are visible. Simultaneously, the outer membrane of the egg changes allowing no other sperm to enter. If it would be the case that two sperms could enter the egg, then too much genetic material would be available and the fertilisation process would in most cases terminate. In mammals, the fertilisation triggers the completion of the meiosis and thus the second polar body forms. There is now only half of the maternal genetic material left in the egg, just the right amount of ge-

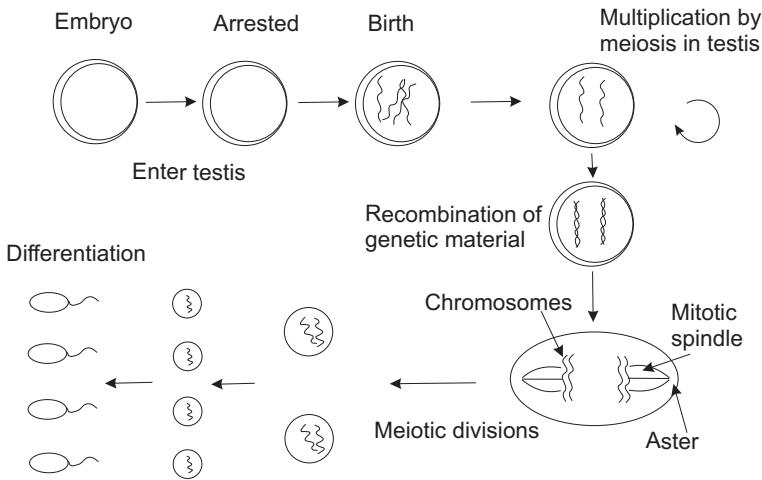


Figure 1.2: Production cycle of sperm, during a mammal's life from embryo to adult.

netic material to form an individual. The female pronucleus is now completely formed. Pronuclear migration takes place towards fusion. Migration is guided by fibrous structures which are called microtubule. They are involved in processes such as cytokinesis and mitosis etc. Microtubules are polymers which can be built up and broken down. They can accomplish both pulling and pushing forces. For more information see Section 4.1. The cytoplasm contains motor proteins which can move along the microtubule, thus enabling transport in this direction. When the pronuclei meet at some point in the egg, their nuclear envelopes start to break down, this is the start for the first mitosis. DNA production takes place separately in the male and female pronuclei and instead of producing a common kernel in the egg, a true diploid nucleus in mammals is first visible in the two-cell stage.

Fertilisation does not happen instantaneously. The pronuclei move quite slowly and speed of the fertilisation differs largely between species. For mammals, the pronuclei migration takes about 12 hours compared to less than one hour for the sea urchin. After the fusion of the genetic material and the first cell division, the cells continue to divide mitotically and form an embryo.

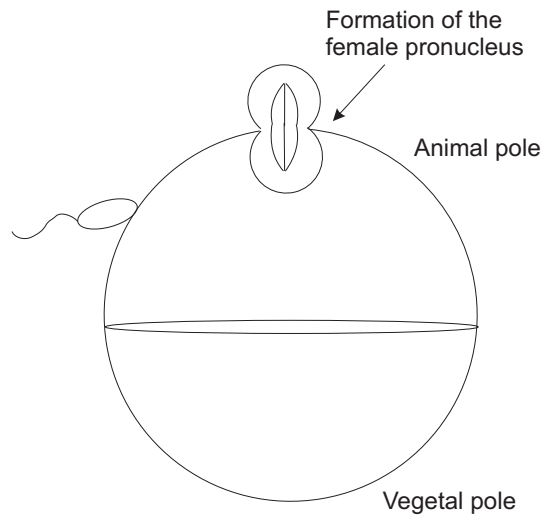


Figure 1.3: A sperm enters the egg (left) and the formation of the female pronucleus is completed. The animal pole is given by the position of the second polar body (This is also referred to as the upper hemisphere of the egg.).

Chapter 2

Data material

Confocal microscopy DIC time-lapse images of mouse eggs were used as data input for the migration model. The imaging method is described more thoroughly in (Plusa et al., 2005). Fertilisation processes in the eggs have been recorded into films of Quicktime format. All this has been done at the Gurdon Institute in Cambridge. These films have been divided into images of tif- and bmp-format for the analysis. From the film sequences, 130 time points (approximately) in each egg's life have been extracted. Each sequential image consists of seven z-scans with $14\ \mu\text{m}$ distance apart; see Figure 2.1. Note that the diameter of a mouse egg is about $80 - 100\ \mu\text{m}$. Each stack covers the egg so that the pronuclei are visible at each time point and their space coordinates can be measured. The width and height of each image pixel at a specific level correspond to $0.37\ \mu\text{m}$. This gives an uncertainty which is quite large in coordinates perpendicular to the image planes (z -axis) compared to the image plane coordinates (x - and y -axes). Sequential images are taken with 5 minutes intervals. Figure 2.2 gives an example of a single time-lapse image at the third z-scan level of one egg. Both the female and the male pronuclei are visible as rather circular structures in the egg. The total number of analysed eggs is four and they are in turn labelled 1, 8, 9, 31.

Figure 2.3 shows an example of two consecutive images shown at the third scan level, or slice of the egg. Also in Figure 2.4 the entire stack of z-scan images can be seen to give an idea of the measuring procedure. What is seen in these figures is the position of the two pronuclei in the egg. The second polar body can be seen in slices 3-7 in figures 2.4(c)-2.4(g) as a bulge at the egg boundary on the left. Also, the male pronucleus is the most in focus at slice 2 which means that it has its centre at this height. It is also somewhat visible in slice 1 and slice 3.

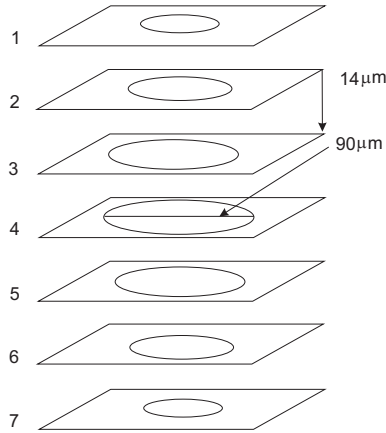


Figure 2.1: Schematic view of the image setting given by the confocal microscopy technique.

The female pronucleus is in its best focus in slice 3, but is also visible in slice 2, slice 4 and slice 5. From these tedious observations the pronuclei's positions can be estimated. Recordings of the pronuclei positions have been carried out by hand, for all three dimensions. The measuring procedure is performed, until the first division, positions are expressed as $\mathbf{m} = (m_x, m_y, m_z)$ for male pronucleus and $\mathbf{f} = (f_x, f_y, f_z)$ respectively for female. Some of the time points have errors in them, e.g. missing slices or inconclusive images, so that they must be discarded. Hence the time points used are not always evenly spaced. The result of this manual measuring procedure can be seen for egg 8 in Figure 2.5.

Some data from two eggs treated with Cytochalasin B (CB) are also available. CB is known to be an inhibitor of microtubule growth and to increase the migration time. Even though this data material is very limited, it allow for an early exploration of the possible consequences of such treatments.

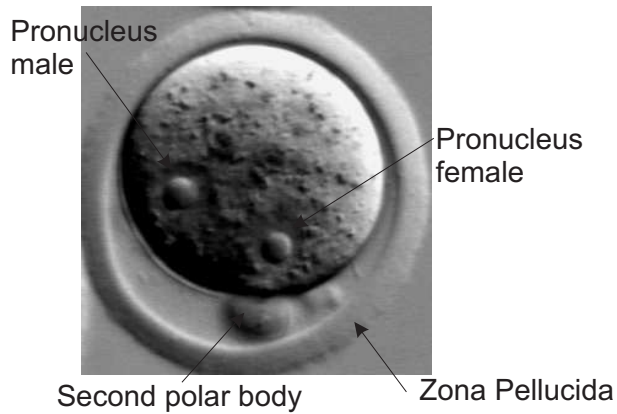


Figure 2.2: An example of a time-lapse image of a mouse egg. The pronuclei are visible, the female pronucleus on the right and male on the left.

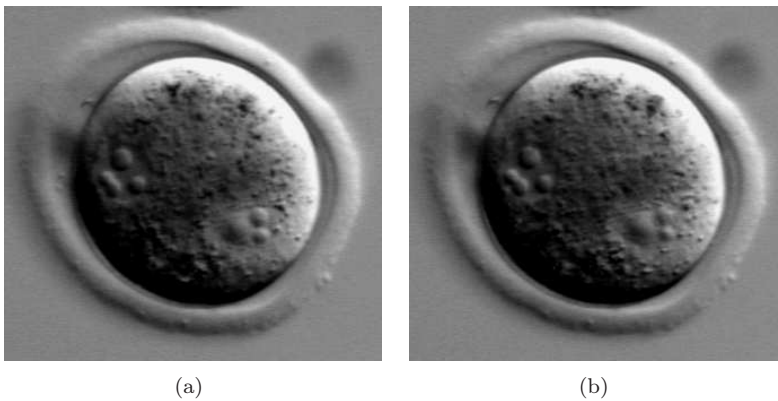


Figure 2.3: Example of consecutive images of Egg 8 at time points 4 and 5. Note that the female pronucleus (left) has its centre at this z-scan level. The male pronucleus is situated a bit higher up in the egg, which can be seen by its contrast being lower than the contrast of the female pronucleus.

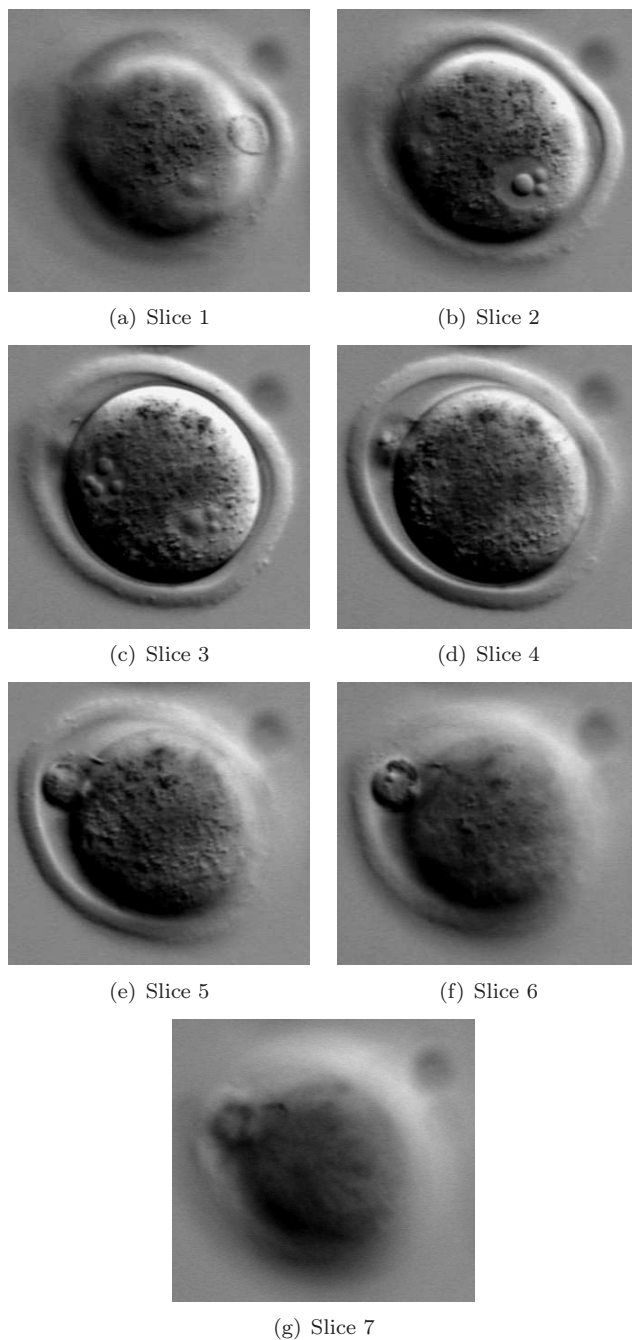


Figure 2.4: Example of z-stack images of Egg 8 at time point 5. The male pronucleus is already visible in slice 1 but has its centre in slice 2. For the female pronucleus it can be seen in slice 2 but is in most focus in slice 3.

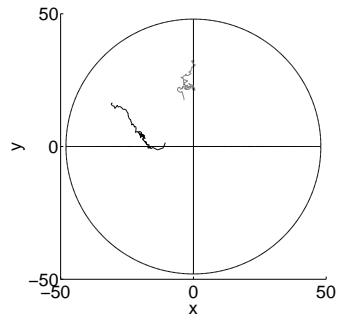
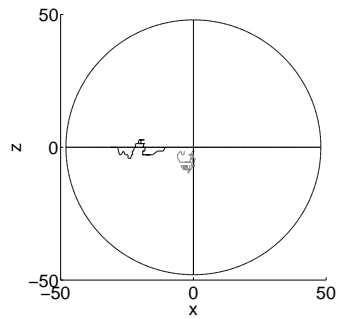
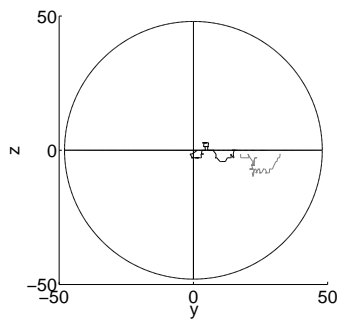
(a) View from xy -plane.(b) View from xz -plane.(c) View from yz -plane.

Figure 2.5: Pronuclei paths for egg 8. The female dynamics are plotted in grey and the male in black.

Chapter 3

Initial data exploration

Currently, very little is known about the pronuclei dynamics in the mouse egg. There exist a few results for the movements in the *C. elegans* egg which is a much simpler organism. Studies where the migration in the mouse egg has been investigated further are for example (Davies and Gardner, 2002), (Hiiragi and Solter, 2004) and (Plusa et al., 2005). The goal here is to learn more about this migration process.

Studying the manual data measurements indicates that the male and the female pronuclei move with essentially the same dynamics; see Figures 3.1 and 3.2. The apparent differences are not the same for each egg. For example, the male dynamics is not always steeper towards the centre than the female, as seen in Figure 3.1. A typical problem with biological data material is the existence of quite large individual differences between each individual (egg). This problem should be eased when gaining more data, but we still want to make some first analyses at this stage. By examining the paths of migration it becomes clear that it is not a simple attractional movement toward the centre, but there seems to be some more complex dynamics involved.

To gain better understanding of the migration process, we have looked at the correlation between the male and the female positions. The initial study presented here is performed to get a feeling for how the data behave. We wanted to know whether the pronuclei are related at all or if they move independently towards the centre. Pronuclei migrate in a 3D world which leads to measurement procedures that account for this property. We have investigated different ways of displaying and analysing the data, such as correlation and phase change tests. First, we will have a look at three different correlation measures.

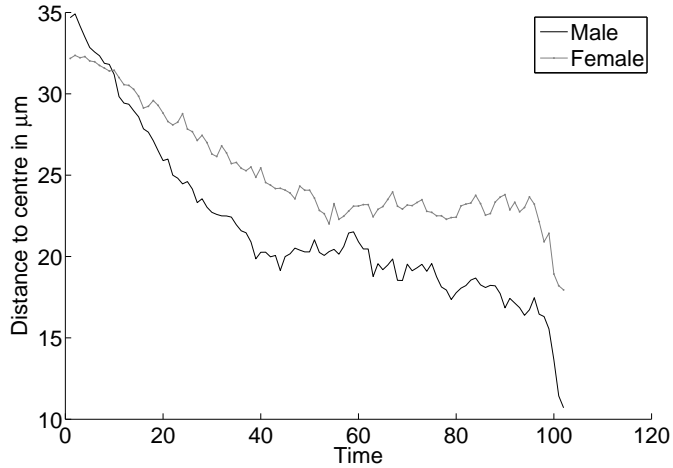


Figure 3.1: Distance in μm from the centre of the egg for the male and the female pronucleus in egg 8 as a function of time. Note that, for this egg it seems like the male pronucleus has a steeper path than the female.

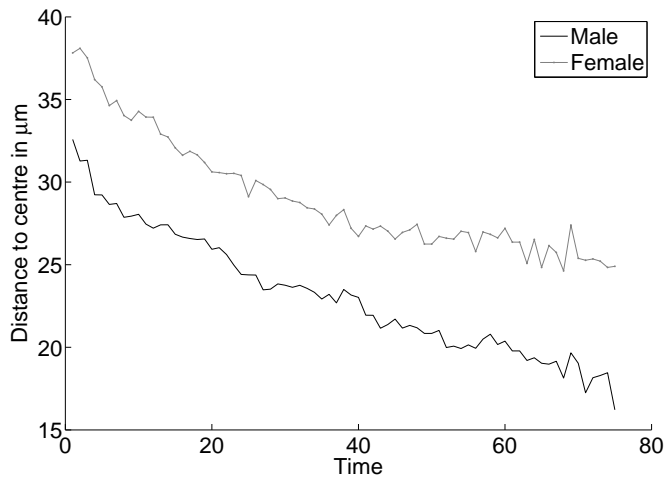


Figure 3.2: Distance in μm from the centre of the egg for the male and the female pronuclei in egg 31 as a function of time. For this particular egg, the pronuclei show very similar dynamic patterns.

3.1 Axis-wise correlation

One way of studying the correlation between the male and female positions is to look at each axis of the migration separately. In our data we have, for each egg, $(\mathbf{m}_1, \mathbf{f}_1), \dots, (\mathbf{m}_N, \mathbf{f}_N)$, where \mathbf{m}_j and \mathbf{f}_j is the j th data measurements of the male and the female position respectively. N is the length of the migration time series. The time series is divided into k parts of size l . If the series is not evenly divisible, the last part may have different length for each egg. For each of the i th part of the data, the correlation between the male and the female x -coordinates is estimated for $1 \leq i \leq k$ by

$$\hat{\rho}_{xi} = \frac{\sum_{j=(i-1)l+1}^{il} (m_{xj} - \bar{m}_i)(f_{xj} - \bar{f}_i)}{\sqrt{\sum_{j=(i-1)l+1}^{il} (m_{xj} - \bar{m}_i)^2 \sum_{j=(i-1)l+1}^{il} (f_{xj} - \bar{f}_i)^2}}. \quad (3.1)$$

Note that $-1 \leq \hat{\rho}_{xi} \leq 1$. The axis-wise correlation is estimated analogously for the y - and z -coordinates. Therefore each axis is investigated separately. Since this method has not really taken care of the multi-dimensionality of the data, it is important to understand which pronuclei movements give rise to certain values of the correlation coefficients. One could think of the migration correlation in the following way:

Correlation near 1: pronuclei move linearly together.

Correlation near -1: pronuclei move towards each other linearly, or they move away from each other linearly.

Correlation near 0: the pronuclei move independently.

In Figure 3.3 is a schematic example of how the correlation coefficient would change depending on the pronuclei's joint movements toward each other.

Unfortunately, the correlation can equal -1 if the distance between pronuclei is increasing. Therefore, we need to assure from the data that this does not occur. If this occurred, it would lead to a non-completed fertilisation. It is not an extremely invasive assumption to assume that the pronuclei move toward each other if we have a long-term trend of negative correlation.

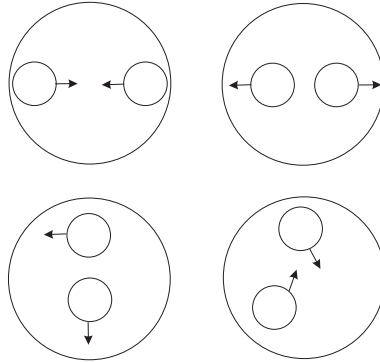


Figure 3.3: Example of different planar correlations possibly occurring during migration: Movements resulting in correlation of -1 (upper row). Zero correlation (bottom left), usually the migration consists of movements over a mix of different dimensions (bottom right). See for instance Figure 3.4.

The correlation coefficients for each axis are then investigated graphically for each egg, see Figures 3.4 and 3.5 for two examples. One can see that something happens with the correlation coefficient at around time points 10-12 since at least for one of the coordinates the correlation coefficient as a function of time is U-shaped and becomes negative. This feature is most apparent for the x -coordinate for egg 8 in Figure 3.5. At first there is an increase of the correlation meaning that the pronuclei move similarly to the centre of the egg. On the other hand after time points 12-30 the correlation starts to decrease in one of the coordinates suggesting that the pronuclei start to move toward each other on this axis. As can be understood from the previous arguments it is often difficult to interpret these correlation curves. Part of the difficulties is due to having to draw conclusions from three curves at once.

3.2 Spherical correlation coefficient

In calculating the correlation coefficient between positional coordinates the issue of having one component for each axis of the movement leads to trouble comprehending the data material. However one would not want to reduce the complexity in a too high extent, since it is important not to lose crucial information about the dynamics. One possibility is to compute the spherical correlation coefficient, (Fisher et al., 1987), (Mardia and Jupp, 1987). The spherical correlation coefficient is a measure of association between sets of vec-

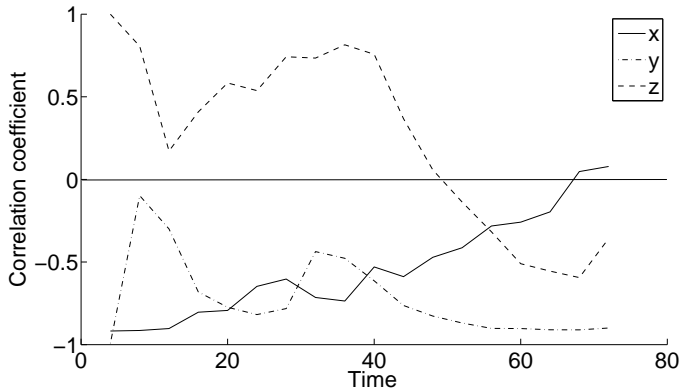


Figure 3.4: Estimated correlation coefficients for each axis of the data between pronuclei positions over time for egg 31. Note the U-shape of the y -axis correlation graph, this might be due to attraction between pronuclei.

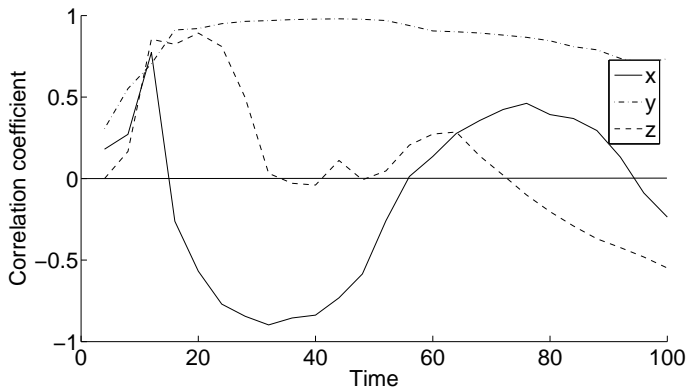


Figure 3.5: Estimated correlation coefficients between pronuclei positions for each axis of the data for egg 8. Note the U-shaped behaviour at around time point 12. Also something additional seems to be happening to the dynamics at time point 40. This may be related to the pronuclei “hooking-up” (see Figure 4.5) and moving to the centre.

tors. We use here the same correlation coefficient as presented in (Fisher et al., 1987). It is interpreted as follows; \mathbf{x} and \mathbf{y} are vectors and the association is perfectly positively for an orthogonal transformation $\mathbf{y}=\mathbf{A}\mathbf{x}$ such that $\det(\mathbf{A})=1$. The vectors are perfectly negatively associated if \mathbf{A} is a reflection matrix (i.e. $\det(\mathbf{A})=-1$). For each of the k parts of the data divided as before, the following quantities are calculated

$$S_{\text{mf},i} = \det \left\{ \sum_{j=(i-1)l+1}^{il} \mathbf{m}_j \mathbf{f}_j \right\} =$$

$$\begin{pmatrix} \sum m_{xj} f_{xj} & \sum m_{yj} f_{xj} & \sum m_{zj} f_{xj} \\ \sum m_{xj} f_{yj} & \sum m_{yj} f_{yj} & \sum m_{zj} f_{yj} \\ \sum m_{xj} f_{zj} & \sum m_{yj} f_{zj} & \sum m_{zj} f_{zj} \end{pmatrix}$$

$$S_{\text{mm},i} = \det \left\{ \sum_{j=(i-1)l+1}^{il} \mathbf{m}_j \mathbf{m}_j \right\},$$

$$S_{\text{ff},i} = \det \left\{ \sum_{j=(i-1)l+1}^{il} \mathbf{f}_j \mathbf{f}_j \right\},$$

for each part i of the data, $i = 1, \dots, k$. Then the correlation coefficient is estimated by

$$\hat{\rho}_i = \frac{S_{\text{mf},i}}{\sqrt{S_{\text{mm},i} S_{\text{ff},i}}},$$

where $-1 \leq \hat{\rho}_i \leq 1$. This estimate for the spherical correlation coefficient is plotted for egg 31 in Figure 3.6. It can be seen that in the beginning the correlation is close to -1 but increases then close to zero. At time 10 it starts to decrease and has some kind of U-shaped behaviour. A U-shape in the spherical correlation is observed in egg 1 too, see Figure 3.7. Furthermore, there seems to be something additional taking place in the egg at time 40, where there is another decrease in the correlation. So, it seems as this measure contains the same information as the correlation coefficients for each axis of the time series but not as strongly expressed. In calculating the spherical correlation, a characteristic which is highly expressed in one axis of movement can easily be smoothed out by one acting in the opposite way for another axis. In terms of statistical significance it can be hard to draw conclusions from these graphs and they are merely a sign of tendency than anything else.

The data are very noisy, but we have chosen not to filter them at all. At this stage of the data analysis when very little is known about the process it seems to be a good choice.

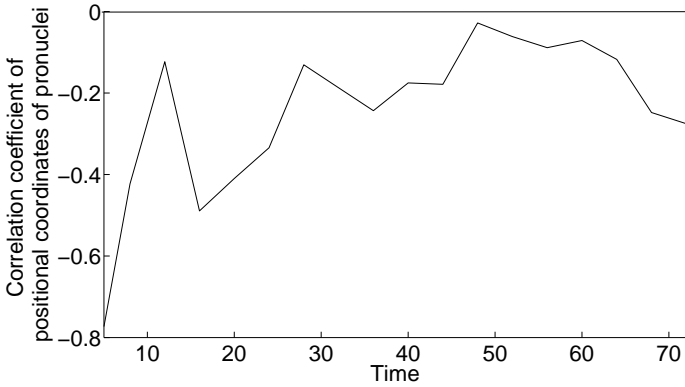


Figure 3.6: Estimated spherical correlation coefficient between pronuclei positions over time for egg 31.

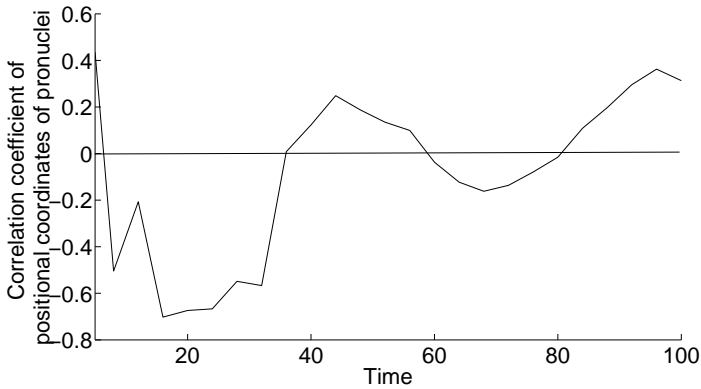


Figure 3.7: Estimated spherical correlation coefficient between pronuclei positions over time for egg 1. Note the change of direction at around time point 8 and 12. Note also that something seems to be happening to the dynamics at time point 40. As discussed for the axis-wise correlation, this might be due to the pronuclei being “hooked-up”.

3.3 A projection measure

To avoid some of the dependency on the starting positions in the egg we have investigated the possibility of using a projection measure. This measure is calculated by simply projecting the movement vector for each pronucleus onto the axis of the distance between them, see Figure 3.8, and then calculating the ordinary one dimensional correlation coefficient of these projections analogue to Equation (3.1). The vector connecting the two locations between the two pronuclei at time t_n , $n = 1, \dots, N$, where t_N is the end of the migration, is denoted $\mathbf{d}(t_n)$. At time t_{n+1} the male and the female pronuclei have moved to positions $\mathbf{m}(t_{n+1})$ and $\mathbf{f}(t_{n+1})$ respectively. To investigate how the migrations in the two processes are related, we take the projections of these new locations of movement. For the female pronucleus we define

$$\mathbf{P}_f(t_n) = [(\mathbf{f}(t_{n+1}) - \mathbf{f}(t_n)) \cdot \hat{\mathbf{d}}(t_n)] \hat{\mathbf{d}}(t_n)$$

and the projection $\mathbf{P}_m(t_n)$ for the male pronucleus is analogue. Here $\hat{\mathbf{d}}(t_n)$ denotes the unit vector in the direction of $\mathbf{d}(t_n)$. The correlation between the female and the male series of projections is calculated in the same way as for the axis-wise correlation in Equation (3.1). The idea with this measure is to try to capture the nature of the dynamics between the pronuclei when they move to a new location. If the migration is in an attractational phase the correlation between these projections should become negative because the projection vectors should be directed towards each other. On the other hand when the pronuclei have hooked-up, this measure should be at some (almost) constant level (disregarding noise factors). The results for our now familiar eggs 8 and 31 can be viewed in Figures 3.9 and 3.10

From these plots we can see that the correlation between the projected components of the direction of movement onto the axis in between the pronuclei starts off as being positive. Then the correlation coefficient decreases and becomes negative, indicating a possible coupling of the male and the female pronuclei. After this the correlation increases again as expected and stabilizes at some level. All the measures show similar behaviour for all eggs, both treated and non-treated eggs. This measure of relation seems a bit easier to interpret since the dimensionality is decreased and it is geometrically easier to understand than the spherical correlation coefficient from the previous section. The different results can be explained by the measures having different sensitivity. It seems though at this point that the projection measure is more suitable than the others. In thinking of how the measures are constructed this is not so strange. The projection measure is looking directly at the resulting movement towards the approaching pronuclei but the other measures are more indirectly taking this into account.

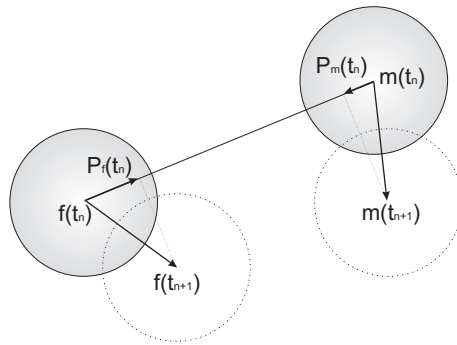


Figure 3.8: The projection measure is calculated by taking the projection of the future positional vector onto the vector between the locations of the pronuclei. The correlation between these projections is analysed to get an understanding of the migration.

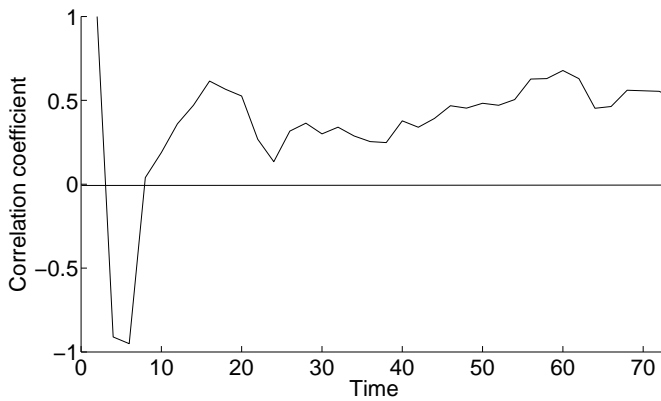


Figure 3.9: The correlation between the projections $\mathbf{P}_m(t_n)$ and $\mathbf{P}_f(t_n)$ for egg 31. The idea of this measure is that a negative correlation can indicate an attractive movement towards each of the pronuclei.

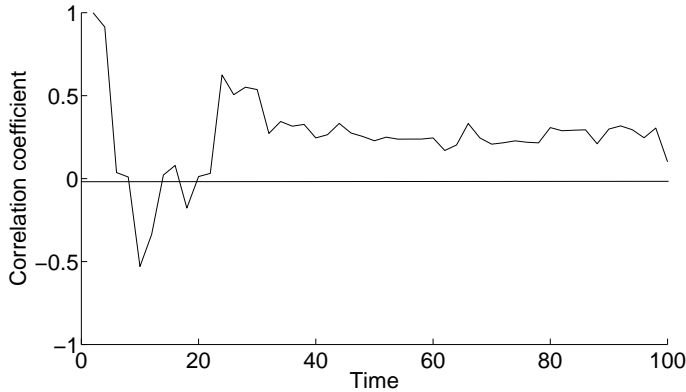


Figure 3.10: The correlation between the projections $\mathbf{P}_m(t_n)$ and $\mathbf{P}_f(t_n)$ for egg 8. Note that the correlation decreases in the beginning of the time series and becomes negative.

3.4 Estimation of phase change by the CUSUM method

The analyses of the previous section indicate that there can be several important events taking place during the migration, the first one at around time point 10-12 and then later events in the time series. To decide if these observations are statistically significant we have performed a change point analysis of the correlations. First, we conclude from the calculations of the correlation coefficients that probably, there have been at least two dynamic changes happening during the migration. Our hypothesis for the changes is that the first change should be when the microtubules have grown long enough and the pronuclei can reach each other. Second change in the dynamics should occur at the point where the astral microtubules of each pronucleus have firmly hooked-up. One can expect a more “independent” behaviour for a while where the pronuclei are not moving that much but are more affected by disturbances of the cytoplasm. The third change would probably occur when the nuclear envelopes of the pronuclei start to break down and the genetic material starts to fuse. For determining the confidence of these events a change point analysis by the CUSUM method, (Page, 1954), has been performed. This method is traditionally used in statistical process control. Note that this analysis is used only for determining if a change has occurred, not what kind of a change it is. In (Taylor, 2000) a combination of CUSUM charts and bootstrapping has been used for detecting change points. The same procedure has been performed

for each of the correlation coefficients calculated in the previous section. Let X_1, \dots, X_n be the time series of one of the correlation measures. In order to detect a change point we follow (Taylor, 2000), and calculate first the average, \bar{X} , of the data values. Then we calculate the cumulative sum of the changes around the mean value as $S_i = S_{i-1} + (X_i - \bar{X})$ for $i = 1, \dots, n$, where $S_0 = 0$.

Since there is a possibility of two (or more) change points in the data, the CUSUM method is first performed on the first part of the data and then on the second part, i.e. the first 10 elements and secondly on the rest of the series. Here, the first part is the part where only one possible change has been observed. An example of a CUSUM chart of the entire time series can be found in Figure 3.11(a). It can be seen that two possible change points have occurred in the data. The curve in Figure 3.11(a) and its zoomed in version in Figure 3.11(b) show whether the observations tend to be above or below the mean value. A descending part shows a tendency for the observation to be below the mean and ascending the opposite. The question is; among all possible CUSUM charts, is the change point produced by the data significant? To investigate this, (Taylor, 2000) used $S_{\text{diff}} = S_{\text{max}} - S_{\text{min}}$, where

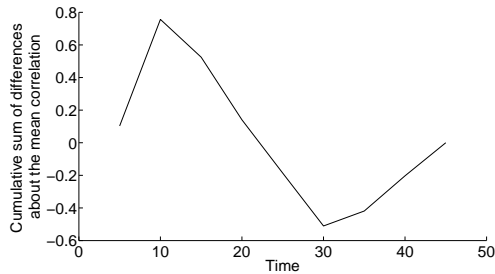
$$S_{\text{max}} = \max_{i=0, \dots, n} S_i \text{ and } S_{\text{min}} = \min_{i=0, \dots, n} S_i,$$

as an estimator for the magnitude of the change. After calculating the test statistic, a bootstrap analysis or rather a permutation test (Manly, 1997) is performed as follows

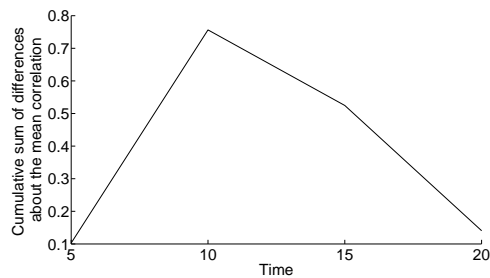
1. The sample (of size n) is randomly reordered B times.
2. For each of the B permuted values the bootstrap CUSUM is performed.
3. As described earlier the maximum, the minimum and the difference is calculated for every bootstrap-sample.
4. Determine how many of the permuted sample differences are less than the difference calculated from the original data.

The confidence level of the change point is calculated as the proportion of bootstrap sample differences less than the difference of the data sample as suggested in (Efron and Tibshirani, 1993). If a change has been detected we take $|S_m| = \max_{i=0, \dots, n} |S_i|$ as a point estimator for the actual time the change has occurred. For each egg the above analysis can be used to conclude if there has been a change in the correlation coefficient and if this change is significant.

The analysis has been performed for all of the measures presented in the beginning of this chapter, however we show only results for the projection measure.



(a) An increasing curve indicates that the current value is above the mean and a decreasing curve indicates that the values being below the mean. Four possible change points can be seen in the plot around times 10, 15, 30 and 36.



(b) The left part of the graph in Figure 3.11(a) is zoomed in.

Figure 3.11: The cumulative sum of the difference around the mean for the projection measure correlation coefficient of egg 8.

Egg	First part	Second part
1	6 (0.84)	32 (1)
9	2 (0.85)	22 (0.99)
8	4 (0.99)	22 (0.99)
31	10 (0.95)	42 (0.99)

Table 3.1: Results of the CUSUM change point estimation for the projection measure. The level of confidence is given for each point in brackets. Note that it can be hard to compare the change point of each egg because of the sperm entry in relation to the second polar body is quite different.

Egg	First part	Second part
Cyto1	6 (0.94)	51 (1)
Cyto2	12 (1)	165 (1)

Table 3.2: Results of the change point estimation for the projection measure for eggs treated with Cytochalasin B.

Results for the four eggs are shown in Table 3.1. In the table we display the time points of the detected changes and their corresponding level of confidence. What is important to realize is that even though the analysis is performed on a time course it is not the specific time of change that is interesting. We are more interested in knowing at which distances pronuclei are able to start to interfere with each other, via microtubule interaction. The CUSUM analysis just gives the largest change point in the particular interval given by the data. We have performed the same analysis on the eggs treated with Cytochalasin B. The results of this are shown in Table 3.2.

Investigating the dependence, especially for directed data, is a difficult problem and a lot of factors need to be taken into account. In this case for instance, the starting positions of the pronuclei have to be well described. Low resolution in the z -axis can also result in that a change point is not discovered. Concerning the restrictive CUSUM method, a big change has to take place for gaining a significant result. CUSUM was originally designed for over-viewing industrial processes and in that case one wants to be certain that a change has occurred before doing something about it. For this analysis we consider it important to take all measures into account to get a complete view of the data, however for intuitive understanding, the projection measure is the most attractive in our opinion. It is probably also the best measure among the three regarding sensitivity and simplification of the data.

Chapter 4

Modelling the pronuclei migration

Microtubules are involved in many cellular processes such as mitosis and cytokinesis; see for example (Gilbert, 2006) and (Wolpert et al., 1998). They are guided from the centrosomes provided by the sperm and the female pronucleus. Along the microtubule, motor proteins can move towards both the plus end (kinein) and the minus end (dynein) of the microtubule. We will in this chapter analyse the components that guide the pronuclei migration a bit further by modelling some of the most important features.

Our aim is to make use of the analysis in the proceeding chapter together with observations of the migration to produce a model that captures the essential features. Furthermore, we will use results from other simpler organisms in the modelling because there are not so many relevant results available for the mouse egg. Manual observations of the migration indicate that not only do the pronuclei move towards the centre of the egg but also towards each other. For example, the experiments by (Hamaguchi and Hiramoto, 2008) show this behaviour for sand dollar (a relative to the sea urchin) eggs. These results and existing models mainly concern the microtubule polymerisation and depolymerisation and the forces that such processes give rise to.

Biomaterials are object to internal stresses and fluctuations and are never really in a state of equilibrium. These stresses and fluctuations are results of active processes and are what make biomaterials unique. Thermal fluctuations and motor fluctuations will lead to diffusion-like movements. Note that motor fluctuations are non-thermal, (Karsenti et al., 2006). Such processes play an

active role in the microtubule life cycle, which in turn consists of the different states: growth, shrinkage and pause. These states give each microtubule the possibility of exerting mechanical forces on its environment. Microtubule generated forces can also be generated by motor proteins, such as dynein and kinesin, which can diffuse within the solvent and become bound to the microtubules. The diffusion process is characterized by isotropic diffusion, (Dogterom et al., 2005). Even though there have been quantitative studies to evaluate the mechanical properties of microtubules, and many properties have been revealed, there is still quite a lot that is unknown. We do not yet fully understand how the microtubules interact with the rest of the cytoskeleton and the cortex of the egg. Let us proceed by giving some background to known mechanics of the dynamical processes of the microtubules.

4.1 Microtubules and the migrating pronuclei

Microtubules are part of the cytoskeleton and they are also the guiding elements of the fertilisation process. They can be seen almost as elastic hollow rods built up by smaller building blocks known as tubulin dimers. Each dimer is in turn made up of α - and β -tubulin polypeptides. Microtubules have one end made up of α -tubulin and the other made up of β -tubulin and become structurally polarized polymers because of this property. The tubes have a diameter of about 25 nm. As already mentioned the microtubule dynamics consist of dynamic processes. The switch between states occurs randomly for different microtubules at different positions; this is known as dynamic instability.

4.1.1 Dynamical mechanics of the migration

We will in this section further pursue the possible strategies currently considered for the centring of the pronuclei during fertilisation. Again we will look into the development of simpler organisms such as *C. elegans* and *Drosophila* in order to get ideas for our model construction. Since few results exist for nuclei positioning we will also make use of known spindle positioning mechanisms. In the studies, among others, (Gachet et al., 2004) and (Gonczy, 2002) it is inferred that astral microtubules exert mechanical forces which lead to spindle movements with respect to cell polarity or cell shape in *C. elegans*, *Drosophila* and vertebrate cell lines. Astral microtubules are radial arrays generated from the microtubule organizing centres provided by the centrosomes. Polymerisation and depolymerisation are processes that influence the mechanical forces generated along an astral microtubule with the help of motor proteins. There-

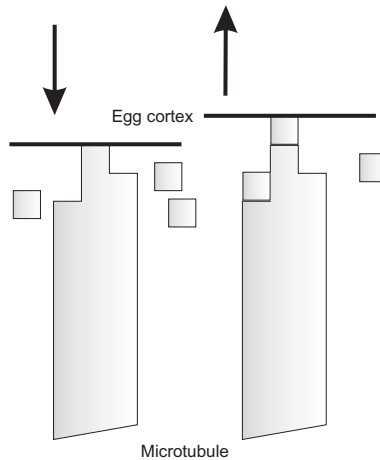


Figure 4.1: Thermal vibrations enable insertion of single microtubule filaments against the egg cortex. A pushing force can be generated, in this way.

fore the microtubule can exert both pulling and pushing forces. We will next discuss how these processes can give rise to the present forces.

It has been shown in in-vivo and in-vitro experiments that tubulin fixed at one end can exert pushing forces, see for instance (Desai and Mitchison, 1997). It has also been studied (in-vitro) how assemblies of microtubules from purified tubulin can produce sufficient pushing forces to position artificial centrosomes. Microtubules do however also behave like elastic rods and buckle when growing too long. This means that the pushing forces are probably mainly existing in small systems or at shorter distances (up to $16 \mu m$), (Gittes et al., 1996). Polymerisation is believed to give rise to pushing forces when the resistance against the microtubule is less than the polymerisation energy. This energy is fluctuating due to thermal noise vibrations of the cortex which gives the microtubule possibility to grow against the cortex and exert a pushing force, see Figure 4.1. This model for the pushing force is the so called Brownian ratchet model (Dogterom et al., 2005).

How depolymerisation of microtubule can lead to pulling forces is much less studied and known than the polymerisation process. It has though been shown in-vitro that the disassembly of microtubule can lead to minus end directed movement, (Dogterom et al., 2005). A schematic picture of how a depolymerising microtubule together with a linking protein may generate a pulling force is shown in Figure 4.2.

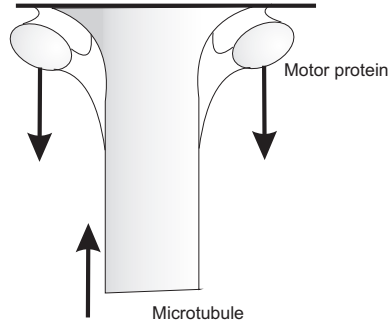


Figure 4.2: One possible way of how depolymerisation together with a motor protein can generate a pulling force. The protein is linked to the egg cortex and binds to the microtubule. While the protein starts to move along the microtubule there will be a movement of the microtubule in the opposite direction.

Generation of mechanical forces is also possible due to so called motor proteins. The proteins related to microtubule dynamics are kinesins and dyneins, (Mallik and Gross, 2004). The force generation is possible because of the motors bind stably to a microtubule and then moving along the actin filaments. Dynein is a minus end directed motor and can generate a pulling force when attached to the egg cortex or somewhere in the cytoskeleton. There has been evidence of higher concentration of dynein at the cortex suggesting that end-on bindings to astral microtubule are possible for pulling-force generation, (O'Connell and Wang, 2000). However, it is still not completely understood how this distribution of dynein in the cell is regulated.

4.1.2 Three available biological models for positioning

Since few results exist for the mechanisms for positioning of the pronuclei, we will make use of ideas of spindle positioning. The mouse egg is almost a spherical system and cannot utilize the specific geometry more than that the geometric centre may serve as a point of equilibrium for the microtubule pushing and pulling. This is to say, that most ideas present are based on the forces being exerted on the cortex and that they balance when the pronuclei have reached the egg centre. For the pushing mechanism the microtubule just polymerizes against the cell cortex. However, when it comes to the pulling mechanisms there currently exist three main models. They all try to take into consideration how the pronuclei can be centred by force exertion of astral microtubules on the cortex.

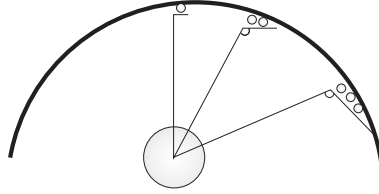


Figure 4.3: The amount of pulling might be dependent on the angle that the microtubule approaches the cortex. A greater angle means that the microtubule does not have to bend as much to attach and pull on to the cortex.

The first model is based on the assumption that the size of force depends on the length of the microtubules, which leads to a net force that is maximal in the direction of the longest microtubule, (Tsou et al., 2003). If a microtubule grows and becomes long, then more motor proteins can bind to it, which leads to a force proportional to the microtubule length. Here, the net force can though result from both cortex anchoring and lateral anchoring in the cytoplasm.

The second model that has been proposed is that the amount of pulling is dependent on the angle that the microtubule approaches the cortex (Vallee and Stehman, 2005). It is thought that the microtubules slide along the cortex until an optimal angle is found. The idea is that if a microtubule approaches the cortex at a perpendicular angle in order to attach and exert force, it would have to bend. In this way the microtubule could attach and transmit more force after sliding along the cortex to find a more efficient binding surface, see Figure 4.3.

The last biological model we will discuss here is one proposed by (Grill et al., 2003). They suggest that there is a limited number of force generators on the cortex, giving that not every microtubule can bind to a force generator. Since the force generators are assumed to be evenly distributed, a displacement from the centre would lead to more force generators being available on one side, leading to a stabilization to the centre.

4.2 Mathematical modelling of the pronuclei migration

The idea of this section is to try to capture some of the features from the previously described biological models in order to model the pronuclei migration.

The migration is described by two stochastic processes $\{\mathbf{m}(t)\}_{t \geq 0}$, $\{\mathbf{f}(t)\}_{t \geq 0}$ for the male and the female dynamics, respectively, both present in \mathbb{R}^3 . We assume that the processes are dependent in some way which is described by a deterministic part of the model. In addition the models include a stochastic noise part. In the following two sections we will describe two models for the deterministic part and then continue with discussing the noise contribution. Finally, the complete models are given.

4.2.1 The basic model

In Chapter 3, we investigated the migration process and found at least two possible mechanisms which were changing over time. According to one of the mechanisms the pronuclei first move independently towards the centre. After some time into the fertilisation process pronuclei can “hook-up” and move in a more restricted way towards the centre and each other for ending up into a phase where the nuclear envelopes break down and the genetic material fuses. Our model will be based on these assumptions. The following presentation of the basic model is an extended version of (Tapani et al., 2009).

In our first model the pronuclear migration is assumed to depend on two forces of attraction, F_C and F_A , or rather two forces that govern the migration processes of the pronuclei. This could be seen as a simple representation of a more complex force compound working on each pronucleus and the environment of the egg. Here, F_C represents attraction towards the centre and F_A represents attraction towards the other pronucleus. For a schematic view of this see also Figure 4.4. Note that in this setting the size of the force F_A is equal in strength for both pronuclei but oppositely directed. Our data are at this stage far from vast, hence it is too uncertain to infer on the differences between the two pronuclei. So for the modelling carried out in this section we assume equality of the dynamics of the two pronuclei.

The intracellular medium is a very crowded environment and pronuclei migration is basically movement at low Reynolds numbers, see for instance (Purcell, 1977) and (Forgacs and Newman, 2005). This leads to a model with only frictional forces and no inertia affecting the pronuclei. Frictional forces are mainly due to the surrounding cytoplasm and cytoskeleton. If only frictional forces are present, the forces should be proportional to the velocity of the pronuclei. The total force compound acting on a pronucleus will then be $F_A + F_C$ and directly related to the velocity.

First, we give a model for F_C , which represents the centring part of the forces acting on the pronucleus. (Kimura and Onami, 2005) use the length-dependent

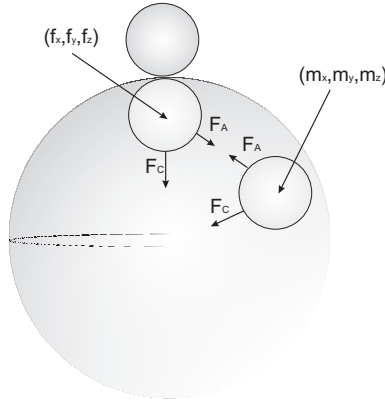


Figure 4.4: Schematic picture of the two attraction forces. The positions of the pronuclei are recorded with three coordinates regarding the position in the image plane (x - and y -coordinates) and estimated height (z -coordinate) in the z -stack.

pulling force as primary mechanism for the *C. elegans* male pronuclear migration. Microtubules that grow towards the cortex of the egg have a limited length, which leads to that the microtubules directed along the centre of the egg are the longest and also give a stronger pulling force than the shorter ones. The pronuclei would then migrate towards the centre. The idea is to have a force that is based on friction and does not blow up at the centre or at the boundary of the egg, when pronuclei are moving against the drag from the cytoplasm. For our first simple model, all the components of the centring will be combined into one centring term and it will not matter which strategy the pronuclei are guided by. We will be able to relate to how large the centring component will be. The two processes $\mathbf{m}(t)$ and $\mathbf{f}(t)$ represent the 3D locations of the male and the female pronucleus respectively. We make the following ansatz for a small change in the positions given a small change in time

$$\frac{d\mathbf{f}_{\text{centre}}}{dt} = C \frac{-\hat{\mathbf{f}}}{(R - |\mathbf{f}| + \epsilon)}, \quad (4.1)$$

$$\frac{d\mathbf{m}_{\text{centre}}}{dt} = C \frac{-\hat{\mathbf{m}}}{(R - |\mathbf{m}| + \epsilon)} \quad (4.2)$$

for the female and the male pronucleus respectively. Where $\hat{\mathbf{f}}$ and $\hat{\mathbf{m}}$ are unit vectors in the direction of \mathbf{f} and \mathbf{m} respectively. Here R is the radius of the egg

and C and ϵ constants that have to be estimated. ϵ assures that the velocity is not too large right at the boundary of the egg. As seen in Equations (4.1) and (4.2) the male and the female centring dynamics are assumed to be similar in this case. The model gives a velocity for the pronucleus which flattens out at the centre of the egg. Though simple, this ansatz has some nice features that can be desirable at an initial modelling state.

Next, we model the attraction force, F_A , of the pronuclei towards each other. This force is modelled by finding inspiration in the theory of electrostatics and charged particles, which seems to be reasonable given the bipolarity of the microtubule. It is desirable that the attraction increases with decreasing distance between the pronuclei, which would represent getting a tighter bond of the microtubule attached to the approaching pronuclei. Given the pronuclei are closer; the microtubule can overlap more and hence get an increase in the strength of the binding of motors along the microtubule. We make the following addition to the earlier ansatz of Equations (4.1) and (4.2) and obtain the final forms of the small changes in the positions, namely

$$\frac{d\mathbf{f}}{dt} = C \frac{-\hat{\mathbf{f}}}{(R - |\mathbf{f}| + \epsilon)} + A \frac{\mathbf{m} - \mathbf{f}}{(|\mathbf{m} - \mathbf{f}|^{\alpha+1} + \gamma)}, \quad (4.3)$$

$$\frac{d\mathbf{m}}{dt} = C \frac{-\hat{\mathbf{m}}}{(R - |\mathbf{m}| + \epsilon)} + A \frac{\mathbf{f} - \mathbf{m}}{(|\mathbf{m} - \mathbf{f}|^{\alpha+1} + \gamma)}. \quad (4.4)$$

Note that, the new term in the male dynamics is equivalent to the female one but added with the opposite sign. The constant γ is added for obtaining a more feasible model for the pronuclei dynamics at the time of meeting so that the velocity does not become too large at this point. The force of attraction is modelled to depend on how big the connecting ‘‘microtubule surface’’ is. If more microtubules are connected it should yield a larger force. The attractional exponent α might be hard to comprehend and to relate to the migration in a biologically reasonable way. Therefore, we will here give a motivation for Equations (4.3) and (4.4) with $\alpha = 2$. In (Payne et al., 2003) it was suggested that higher density of microtubule connected to the other pronucleus yields a higher force. Given that the distance between the approaching pronuclei is ρ , and the radius of a pronuclei is r , we get from similarity that $\frac{r}{h} \approx \frac{\rho}{r}$; see Figure 4.5. Here h is the height of the intersecting microtubule area of one pronucleus. This area ($\approx \pi h^2$) is then proportional to the quantity $\frac{r^4}{\rho^2}$, and hence the resulting force is proportional to one over the squared distance between the pronuclei. This is the same as having $\alpha = 2$ in Equations (4.3) and (4.4). In Chapter 5 we will explain how to estimate the parameters of this model.

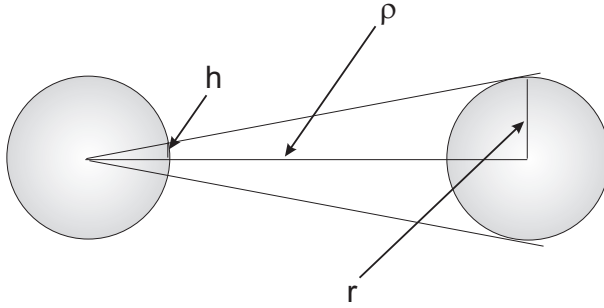


Figure 4.5: Illustration of how the attraction between pronuclei is modelled. The attractive force is modelled to depend on the connected area of microtubules sent out. Similarity yields a force proportional to $1/\rho^2$, where ρ is the distance between the pronuclei.

4.2.2 A refined model

In our second attempt in modelling the dynamics we will try to take the properties of pushing and pulling into greater account. Quantitative studies, (Kimura and Onami, 2005), (Dogterom et al., 2005), (Nédélec, 2002), suggest that a single microtubule behave as an elastic rod and that movement takes place through decreasing velocity for an increasing load. The microtubule clings to the cytoskeleton in a homogeneous way and the number of motor proteins that guide the movement should be proportional to the length of the microtubule. The first described property leads to an elastic rod exerting a pushing force until it reaches its maximum and bends. This will lead to an increasing force that has an upper limitation and the force should decrease with the length of the microtubule. Because of this the pronuclei will be pushed away from the cortex. The second property leads to a combined pulling force since it is both cortical bound dynein and dynein that is uniformly distributed throughout the cytoplasm that binds evenly to the microtubule and exerts pulling forces. The pulling force will be proportional to the length of the microtubule and will lead to a centring force since the resultant of forces on the pronuclei will be balanced in the centre of the egg. In the same way as for the previous attempt in Chapter 4.2.1, we will model the velocity to be proportional to the forces. We keep the second term between the pronuclei as in Equations (4.3) and (4.4) but modify the centring term, with the reasoning above in mind, as

$$\frac{d\mathbf{f}_{\text{centre}}}{dt} = -(C_{\text{push}}e^{-(R-|\mathbf{f}|)})\mathbf{1}_{(R-|\mathbf{f}|<d_{\text{buckle}})} + C_{\text{pull}}|\mathbf{f}|\hat{\mathbf{f}}, \quad (4.5)$$

$$\frac{d\mathbf{m}_{\text{centre}}}{dt} = -(C_{\text{push}}e^{-(R-|\mathbf{m}|)})\mathbf{1}_{(R-|\mathbf{m}|<d_{\text{buckle}})} + C_{\text{pull}}|\mathbf{m}|\widehat{\mathbf{m}}. \quad (4.6)$$

Here C_{push} , C_{pull} , A , γ and α are constants to be estimated and $\mathbf{1}_{(\cdot)}$ denotes an indicator function. Furthermore d_{buckle} denotes the distance from the cortex at which the microtubule buckles. In Equations (4.5) and (4.6) the term after the constant C_{push} is seen to model the pushing behaviour of the microtubules and the term after the constant C_{pull} the pulling. In this way the first component of the centring part is modelled to vanish at the buckling distance, which means that it will represent the behaviour of an elastic rod pushing against the cortex. The second component will balance out in the middle of the egg, as to describe the pulling resultant exerted in all directions. Together these components model both the pushing and the pulling mechanisms of the microtubules.

4.2.3 Dissecting the noise

In modelling the noise it is important to take into account the underlying mechanisms of the cause of the noise. What are the dynamic processes in the migration that give rise to what we perceive as noise? The environment in the mouse egg is not simple fluid material. It is on the contrary quite complex and the microtubule guided migration meets a resistance from the surrounding cytoplasm. This leads to natural variation in the data which needs to be taken into account in the model. Also, since we know very little about the migration, the noise term contains everything not explained by the deterministic part of the model.

Our first attempt is to model the random variation using Brownian motion such as

$$\begin{aligned} \sigma d\mathbf{B}(t) &= \sigma(\mathbf{B}(t+dt) - \mathbf{B}(t)) = \\ &= \sigma(B_x(t+dt) - B_x(t), B_y(t+dt) - B_y(t), B_z(t+dt) - B_z(t)), \end{aligned}$$

where $B_{\cdot}(t) \sim N(0,1)$ independent for the x -, y - and z -coordinates. Here we have assumed that the egg is spatially homogenous and that the standard deviation is constant. This makes it easier to estimate the variation of the noise since then the variation is assumed to be equal for all axes and not changing with position in the egg.

However this is not perfect. First of all, the largest source of the noise is the measurement errors. The positions are measured by hand which makes them subjective, especially the z-scan coordinate, where the uncertainty is high. Secondly, the egg is exposed to thermal noise which influences the cytoskeleton and the egg cortex. This is an important process since it makes it possible for the insertion of new filaments on the microtubule plus end when growing towards the cortex and exerting pushing forces. Thirdly, noise will be generated by the invasive measuring procedures and the recordings with the confocal microscopy. Fourthly, we know that the binding and unbinding of motor proteins along the microtubule lead to a diffusion like movement in positioning the centrosomes, which will also cause some of the noise. Switching between growth, shrinkage and pause in the microtubule growth cycle occurs randomly. Finally, the standard deviation of the noise could be written as

$$\sigma = \sigma_{measure} + \sigma_{thermal} + \sigma_{light} + \sigma_{motor} + \sigma_{dynamic} + \sigma_{unknown},$$

where $\sigma_{measure}$ is the standard deviation of the measurements errors, $\sigma_{thermal}$ the thermal noise standard deviation and σ_{light} the standard deviation of the noise from the microscopy measuring technique. Furthermore, σ_{motor} is the standard deviation resulting from the isotropic diffusion of the motor proteins and $\sigma_{dynamic}$ is the standard deviation of the noise consisting of the dynamical events in the microtubule life. Finally, $\sigma_{unknown}$ is the standard deviation of the still unknown pieces of the migration. All in all, the components listed above give rise to quite different types of noise with need of varying models for the standard deviation. In this first modelling attempt we have though assumed a constant overall standard deviation even though we know it is far from correct.

4.2.4 The complete models

We are now ready to state our complete models for the pronuclei migration. With noise added to the models of Chapters 4.2.1 and 4.2.2. For the first model this yields the following pair of stochastic differential equations, SDE, model for the dynamics of the pronuclei

$$\begin{cases} d\mathbf{f} &= \left[C \frac{-\hat{\mathbf{f}}}{(R-|\mathbf{f}|+\epsilon)} + A \frac{\mathbf{m}-\mathbf{f}}{(|\mathbf{m}-\mathbf{f}|^{\alpha+1}+\gamma)} \right] dt + \sigma d\mathbf{B}(t), \\ d\mathbf{m} &= \left[C \frac{-\hat{\mathbf{m}}}{(R-|\mathbf{m}|+\epsilon)} + A \frac{\mathbf{f}-\mathbf{m}}{(|\mathbf{m}-\mathbf{f}|^{\alpha+1}+\gamma)} \right] dt + \sigma d\mathbf{B}(t). \end{cases} \quad (4.7)$$

Analogously, we get for the refined model the following coupled SDE

$$\left\{ \begin{array}{l}
 d\mathbf{f} = \left[- (C_{\text{push}} e^{-(R-|\mathbf{f}|)}) \mathbf{1}_{(R-|\mathbf{f}| < d_{\text{buckle}})} + C_{\text{pull}} |\mathbf{f}| \right] \widehat{\mathbf{f}} \\
 \quad \quad \quad + A \frac{\mathbf{m} - \mathbf{f}}{(|\mathbf{m} - \mathbf{f}|^{\alpha+1} + \gamma)} \right] + \sigma d\mathbf{B}(t), \\
 \\
 d\mathbf{m} = \left[- (C_{\text{push}} e^{-(R-|\mathbf{m}|)}) \mathbf{1}_{(R-|\mathbf{m}| < d_{\text{buckle}})} + C_{\text{pull}} |\mathbf{m}| \right] \widehat{\mathbf{m}} \\
 \quad \quad \quad + A \frac{\mathbf{f} - \mathbf{m}}{(|\mathbf{m} - \mathbf{f}|^{\alpha+1} + \gamma)} \right] dt + \sigma d\mathbf{B}(t).
 \end{array} \right. \quad (4.8)$$

Chapter 5

Parameter estimation

We would like to evaluate and to use the models from the previous chapter to draw conclusions of how well they describe the data. To able to do so we aim in this chapter to estimate the parameters of the models from the available data. The differentials of the positional coordinates are calculated by simple first order approximations. The data consist of four normal eggs and two treated with Cytochalasin B. All four normal eggs are considered with equal weights and the same for the two eggs treated with Cytochalasin B, but the normal and the treated eggs are analysed separately. Female and male measurements are taken to be from similar dynamics, meaning having same values of the parameter estimates, consistent with our models. Also it is assumed that the variance is the same for both pronuclei.

The method used in the parameter estimation is the nonlinear least squares method of Gauss-Newton line search type, (Moré, 1977). It finds a minimum of the sum of squared residuals given by the set of parameters. The implementation of the estimation method is performed in MATLAB. The method minimizes the following sum

$$\min_p (f(p)) = f_1(p)^2 + f_2(p)^2 + \dots + f_n(p)^2$$

where

$$f_i(p) = v_{\text{data},i} - v_{\text{model},i}$$

is the residual of the speed ($v_{\text{data},i}$) of a pronucleus and the speed from the model prediction ($v_{\text{model},i}$) at data point i . Here p denotes the parameter set that the sum of squared residuals should be minimized over. Parameter

C	0.051R (0.050R,0.052R)
A	0.0941R (0.09400R,0.0970R)
ϵ	$2.0 \cdot 10^{-6}R$ ($9.0 \cdot 10^{-8}R, 2.1 \cdot 10^{-6}R$)
γ	$5.4 \cdot 10^{-6}R$ ($4.6 \cdot 10^{-16}R, 9.2 \cdot 10^{-6}R$)
α	1.81 (1.78,1.88)
σ	0.0205R (0.0200R,0.0210R)

Table 5.1: Parameter estimation for the first model. Confidence intervals at the 95%-level are shown in brackets, the intervals are computed by using the jack-knife method on the residuals. R is the radius of the egg.

estimates should be seen only as an indication of what to expect, since data are so limited. The standard deviation of the noise term is estimated from the data after removal of the parts explained by the respective models.

5.1 Results for the basic model

In this section we will present the results of the parameter estimation considering the basic model 4.7. The estimated parameters are C , A , ϵ , γ and α . Finally, we will also present an estimate of the standard deviation of the noise, σ . First we will give the results for the untreated eggs, and then the results for the eggs treated with Cytochalasin B. Using the above mentioned least squares method we obtain the results shown in Table 5.1.

The attraction constant, A , becomes almost twice of the centring constant, C . So for our data it seems like the attraction plays a central role. Cut-off parameters ϵ and γ are considered so small that they can be assumed to be zero even though they are significantly larger than zero. Worth mentioning is that we come very close to the expected value of 2 for the exponent α . We also examined what the consequences of the Cytochalasin B treatment are for the model parameters. The parameters for the pronuclear migration are reestimated for the Cytochalasin B data with the same method as above. Results are shown in Table 5.2. Since Cytochalasin B hinders the microtubule to grow, the rate of migration would decrease.

As expected the values of the parameter estimates for the centring and attraction force, C and A , become smaller than for the untreated eggs. The

C	$4.62 \cdot 10^{-16}\text{R}$ ($4.60 \cdot 10^{-16}\text{R}, 5.00 \cdot 10^{-16}\text{R}$)
A	0.020R (0.019R, 0.021R)
ϵ	$4.61 \cdot 10^{-16}\text{R}$ ($4.60 \cdot 10^{-16}\text{R}, 4.64 \cdot 10^{-16}\text{R}$)
γ	$4.64 \cdot 10^{-16}\text{R}$ ($4.62 \cdot 10^{-16}\text{R}, 6.70 \cdot 10^{-16}\text{R}$)
α	2.05 (2.04, 2.06)
σ	0.0048R (0.0045R, 0.0049R)

Table 5.2: Results of the parameter estimation for the first model for eggs treated with Cytochalasin B.

centring force seems actually to become so small as it can be considered zero, but significantly larger than zero. Again the cut-off parameters are considered being so small so they can be rounded off to zero. More important than the actual results for our model is that it indicates a possibility of using parameter estimates from data of diverging characteristics in simulation studies. Results from these simulations could in turn be used for testing if measuring techniques or treatments used are too invasive.

5.2 Results for the refined model

In this section we will present the results from the parameter estimation for the refined model 4.8. We use the same estimation scheme as before in the previous chapter. The parameter estimates are shown in Table 5.3. However, the parameter d_{buckle} is set to $16 \mu\text{m}$ since in vitro measurements of the microtubule buckling length, (Gittes et al., 1996), have shown that lengths up to $16 \mu\text{m}$ are possible.

Interesting to notice is the relation between the pushing and the pulling centring force constants, C_{push} and C_{pull} . The pulling mechanism is in several studies considered to be the primary mechanism for pronuclei centring, (Kimura and Onami, 2005), (Payne et al., 2003), (Dogterom et al., 2005). Our model shows the same behaviour. The attraction constant, A , becomes smaller than for the basic model and of the same size as the centring constant for the pulling mechanism. Also the cut-off parameter γ does not become as small as for the previous model, however the confidence interval is quite broad. The exponent α is conclusive with the earlier reasoning and estimations. Parameter estimation for the eggs treated with Cytochalasin B is not possible for this model since

C_{push}	$8.8 \cdot 10^{-8}\text{R}$ ($1.6 \cdot 10^{-10}\text{R}$, $1.4 \cdot 10^{-5}\text{R}$)
C_{pull}	0.000115R (0.000110R , 0.000123R)
A	0.00010R ($6.1 \cdot 10^{-5}\text{R}$ R, 0.00054R)
γ	0.10R ($8.8 \cdot 10^{-8}\text{R}$, 0.11R)
α	2.00 (1.99 , 2.04)
σ	0.0202R (0.0201R , 0.0204R)

Table 5.3: Parameter estimation for the refined models.

we do not have data of pronuclei migration close to the cortex of these eggs. Therefore, we are not able to estimate the size of the pushing mechanism.

Chapter 6

Simulation study

In order to visualize the consequences of the models of Chapter 5 and to see how well they describe the data, simulations have been performed and the simulated pronuclei dynamics have been plotted. For initial positions of the male pronucleus in relation to the second polar body, the future positions for the pronuclei have been calculated in successive time steps. For each time step the next spatial positions have been calculated from the models by using a simple forward Euler scheme. For one specific egg, the starting coordinates have been used to run a couple of simulations. The result is shown in Figures 6.1(c) and 6.1(e). The actual trajectories recorded are plotted in Figure 6.1(a). The model succeeds to mimic some of the behaviour that is observed. However there seems to be a larger spread in the simulated data than in the real ones. This may be a feature of the analysed eggs having quite large individual variation.

In Figures 6.1(d) and 6.1(f) two realizations of the refined model are plotted, which are to be compared with the data plot shown in Figure 6.1(b). The same feature observed for the basic model is observed for the refined. It seems as the variation of the data is not captured successfully, however the pronuclei migrate toward each other and to the centre.

Monte Carlo simulations of the dynamics are carried out ten thousand times to produce a distribution of trajectories for the pronuclei. At each simulation the meeting orientation is recorded, or rather the angles that specify the vector between the centre points of the approaching pronuclei, see 6.2. Simulations of this kind could in turn provide initial conditions for future models regarding cleavage of the egg. One can in addition analyse these distributions for different given sperm entry points to get a picture of how the migration behaviour of the

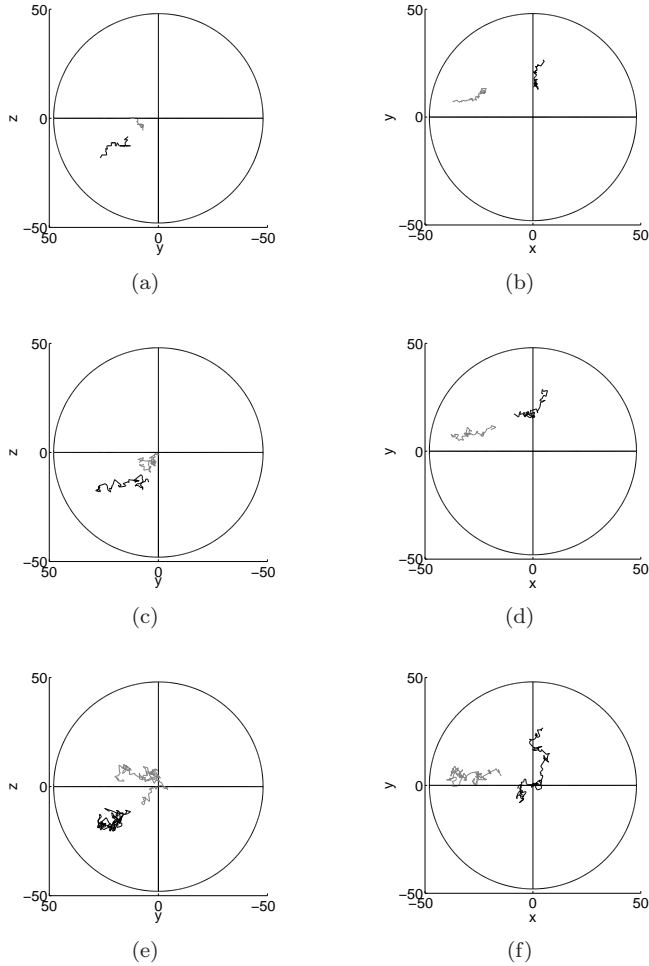


Figure 6.1: Top row, plot of manual data for egg 31 in the yz -view and xy -view respectively. Middle and bottom left: plot of simulations from the basic model, yz -view. The male trajectory is plotted in black and the female trajectory in grey. As initial positions for the pronuclei are the starting positions of egg 31 used. Middle and bottom right: plot of simulations from the refined model, xy -view.

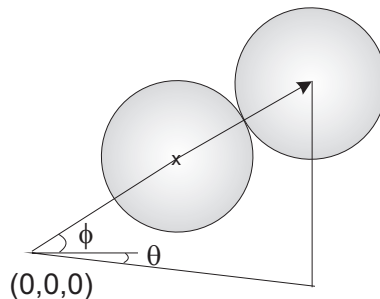


Figure 6.2: The meeting orientation is specified by an elevational and an azimuthal angle.

pronuclei might change. The motivation for these distributions comes from the measurements performed in (Plusa et al., 2005), where the first division plane of the egg was recorded in relation to sperm entry. Measurements were carried out in one dimension; we wanted to show that it is informative to obtain a 2D distribution.

The two dimensional distribution for both the azimuthal (θ , the angle around the “equator” of the egg) and elevational (ϕ) angle of the vector between the pronuclei are recorded, see Figure 6.3. The polar body is always at the “north pole” and the sperm entry point (SEP) is varied in the elevational angle but held at azimuthal angle 0° , “Greenwich meridian”. The sperm entry points used in this study are at the elevational angles of 45° , 0° and -45° . Note that azimuthal angle of 180° , is equal to azimuthal angle of -180° . The results for the first model and the parameter estimates for both non-treated and Cytochalasin B data are shown in Figure 6.4. Red colour means high counts and blue low.

According to the simulations of this model a sperm entry further from the second polar body would introduce a wider spread of where the pronuclei meet and possibly also a wider spread of the cleavage plane. The mean of the angular distributions seems to be positioned at the same place for the different sperm entry points. In analyzing the histograms of Figure 6.4 it is realized that the spread is narrower in the distribution for the eggs treated with CB than for the untreated eggs. According to the simulations a lower centring force gives a smaller spread in the positions where pronuclei meet. If these positions are important in the future cleavage of the egg this may be an indication of an undesired invasiveness of the treatment. The results of the simulations from this model clearly give higher variation of the outcomes of the migration in the egg not treated with Cytochalasin B than in the treated ones. This property can be related to the reduced complexity of the model with the CB parameter

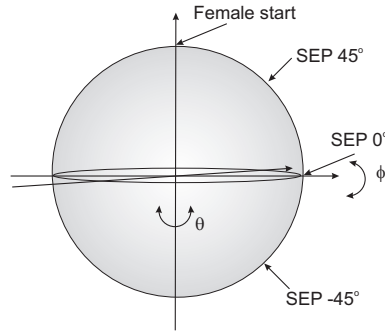


Figure 6.3: For a fixed SEP, 10000 simulations are carried out. For each one the azimuthal angle, ϕ , and the equatorial angle, θ , are recorded.

estimates. Also we can draw the conclusion that for this model the meeting position is highly dependent on where the pronuclei start in relation to each other.

In Figure 6.5 results from Monte Carlo simulations of the refined model are presented in the same way as for the basic model. The same behaviour as for the basic model can be seen for different sperm entry points, i.e. wider spread for sperm entry further away from the polar body. However, for the simulations of this model we get a wider spread in meeting positions of the pronuclei than for the basic model. We think that this might be due to the extra complexity added at the centre of the egg. Comparing the basic model and the refined model, the centring mechanism and the pushing mechanism are similar. Close to the centre the centring force is very small in the basic model and for the refined model this term has vanished by the parameter estimation. However, in the refined model we still have the pulling force, which adds to the movement even close to the centre. This might be the reason for the larger variation.

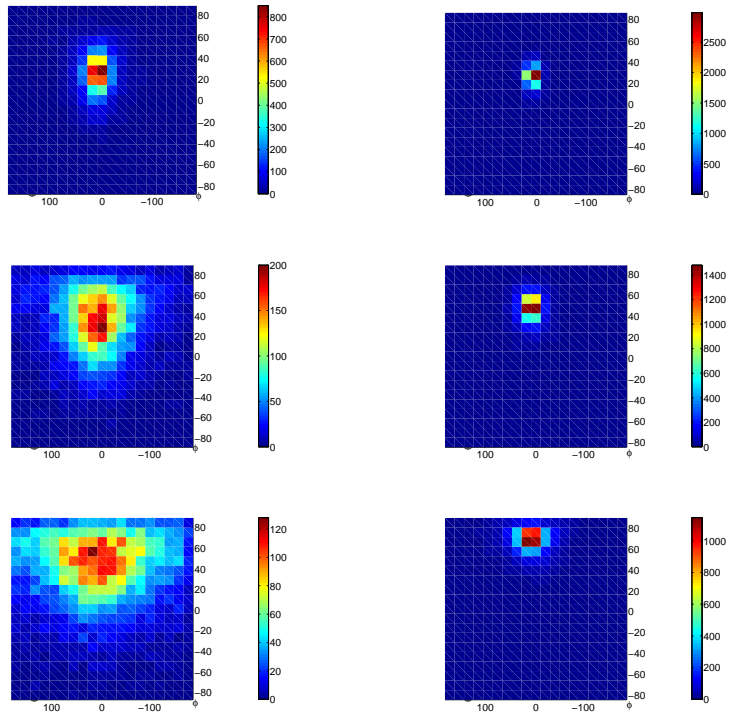


Figure 6.4: Distributions of pronuclei meeting positions from the Monte Carlo simulations for the basic model. The model simulations with parameter estimates of non-treated eggs are on the left column and simulations with CB estimates on the right column. Top row: SEP at 45° ; middle row: SEP at 0° ; and bottom: sperm entry at -45° .

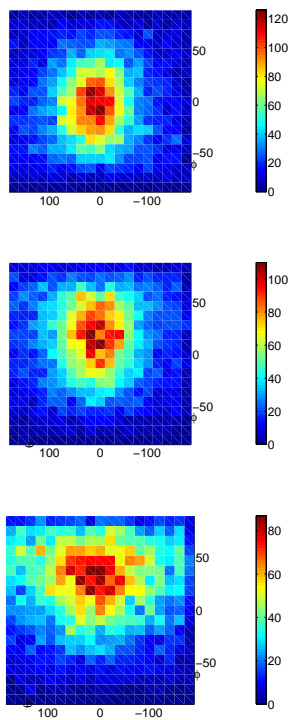


Figure 6.5: Distributions of pronuclei meeting positions from simulations of the refined model. Top: sperm entry at 45° ; middle: sperm entry at 0° ; and bottom: sperm entry at -45° .

Chapter 7

Discussion

This thesis investigates the pronuclei dynamics with both graphical methods, different statistical measures and utilizes a method from statistical process control to examine possible changes of the characteristics of the dynamics during fertilisation. We have started by analysing data of sequential confocal images of the pronuclei migration from the start of the fertilisation until the pronuclei meet somewhere in the egg. These analyses have shown that the characteristics of the dynamics change at least once over time. Such events can be explained by astral microtubule hooking-up with each other at a certain range to produce an attractional phase in the migration between the pronuclei and later when the nuclear envelope starts to break down. The measures tested in Chapter 3 were a starting point for trying to take on the difficult problem of performing analyzes in three dimensions. As mentioned in the introduction, previous studies have discarded eggs where migration takes place in 3D. It was considered here that the correlation coefficient between pronuclei positions axis by axis, is giving a lot of information on the process. However, this measure is hard to grasp and it requires good knowledge about the data. The spherical correlation on the other hand merged the axes of movement together but tended to smooth out the information in the data to a too large extent. Looking at these measures and comparing them, it becomes obvious that the measures seem to capture some events differently and agreeing on others. For instance, the axis-wise correlation and the projection measures seem to agree for some eggs on the early events. On the other hand, for the last part of the data the measures differ a lot. The reason for this is that each of the measures finds all change points, however the relative size of the change is not the same. Our results show that the projection measure is quite easy to comprehend since we only

analyse the movements in the direction of the distance between the pronuclei. Also, the positional correlation is a measure that is dependent on where the pronuclei start in relation to each other. If they start at opposite sides of the egg and move towards the centre of the egg we would get a quite large negative correlation all the way. The results can be interpreted into events of the migration, such as attraction.

We also introduced two models for the pronuclei migration in three dimensions for the mouse egg and described how they can be applied to actual data of fertilised mouse eggs. First, a basic model was presented. This model aims to describe the migration at a mechanical level. It is based on a few simple assumptions and is meant to serve as the starting point for more complex and biologically more relevant models. The model was even reduced further given the data. Furthermore, we give a motivation for having a certain expression for the attraction between the pronuclei which is in turn specified by estimating the parameters from the data. Secondly, we presented a refined model where pushing and pulling on the egg cortex, two important mechanisms of pronuclei centring were modelled. Parameter estimation was in this case consistent with other existing studies which found the pulling mechanism to be primary, (Kimura and Onami, 2005), (Nédélec, 2002) and (Dogterom et al., 2005). Both models are of SDE type and model migration in the mouse egg in space. The noise of the dynamics was modelled using Brownian motion with a constant standard deviation and independence between the axes of motion. Given the complexity of the mouse egg this can seem far from perfect. However, at this point when the available amount of data being small we have made this choice. We hope that we in the future can model the different mechanisms contributing to the noise in a more thorough way. Especially, it would be interesting to look into the microtubule life cycle containing switches between the states growth, shrinkage and pause, and incorporate this in the noise model.

Simulations from both models were carried out to compare with the manual data measurements. The same initial values as in the data were used in the model simulations for all eggs. Inspection of these realizations showed that the main direction seems consistent and the pronuclei migrate towards each other and to the centre of the egg. However, the variation of the data seemed not to be mimicked very well. To visualize the effects on the meeting points of pronuclei of the models, several simulations were performed and in each we recorded the meeting point of the pronuclei. In this way we can show that having a migration described by a few processes but driven by noise can lead to variation in the meeting positions. If this in turn has an effect on the orientation of the future cleavage plane of the egg, it is an important indication. So in a way, randomness of the cell system can lead to randomness in cell fates even though we have a somewhat determinative behaviour in the beginning. It

was interesting to see that the refined model introduced a larger spread in the meeting points of the pronuclei than the basic model. We think that this fact come from the extra complexity of the model close to the centre of the egg. The simulations were also made to show as a complement to measurements carried out of eggs in 2D, where the cleavage plane in relation to sperm entry was recorded, (Plusa et al., 2005). Here we simulate meeting points in relation to different sperm entry points with the third dimension taken into account and show that it gives some extra information.

We also had data of eggs treated with Cytochalasin B, known to inhibit microtubule growth. Model parameters for the basic model were fitted to these data as well and simulations were carried out to compare with the data of non-treated eggs. Our results indicate that the Cytochalasin B treatment affects the pronuclei migration, which is something we would like to investigate further with more data at hand. However, we did not have data that made it possible to estimate parameters for the refined model. It would be interesting to see what effect the CB treatment would have on the pushing and pulling mechanism.

The largest problem so far has been that the available data are so limited. We would like to have a variety of eggs where pronuclei start at uniformly distributed distances from each other. In order to test whether the starting positions do infer on the meeting plane and on the later state of cleavage of the egg. Individual differences between the eggs are quite large and it would be interesting to see if we could say a bit more on how the “mean” egg behaves during fertilisation, and to increase the accuracy of the estimation. To be able to do so, we also need to increase the number of eggs in our study. We have investigated how Cytochalasin B affects the model parameters. The values of the model parameters could be used to test the invasiveness of different treatments and perhaps also the imaging technique. As the imaging technique continuously improves it is possible to have a better resolution in both the image plane data and a smaller distance between the z-scan levels. Even though individual differences are large, it is our opinion that z-scan resolution is still the biggest limitation of the data. However, one should not push this in a too great extent. It is important not to use imaging techniques that affect the migration in an undesired way through light exposure, as the egg is a sensitive system.

Future models should contain a more thoroughly modelled noise term. This should take care of the dynamics of the microtubule growth cycle, thermal vibrations of the egg cortex, the binding and unbinding of motor proteins along the microtubule and the errors from the measuring technique. The manual measuring procedure for instance, is not an easy task but something that should

be performed by an experienced person with good knowledge of the migration process. It is also our intention to make use of better analysis methods such as semiautomatic or automatic image analysis methods for tracking the pronuclei in the image sequences. In order to minimize these sources of errors as much as possible and to be able to analyse pronuclei trajectories more efficiently. Modelling should also be carried out to follow consistently with developmental biology literature. A challenge for the future is to model the cytoskeleton on a smaller level. The microtubules that govern the migration are a part of and cling to the cytoskeleton when engaged in the fertilisation. Understanding these mechanisms can be the key to explain the movements of the pronuclei.

Bibliography

- Davies, T. and Gardner, R. (2002). The plane of first cleavage is not related to the distribution of sperm components in the mouse. *Human Reproduction*, 17(9):2368–2379.
- Davies, T. and Gardner, R. (2003). Philosophical Transactions: Biological Sciences. *Human Reproduction*, 358(1436):1331–1339.
- Desai, A. and Mitchison, T. (1997). Microtubule polymerization dynamics. *Annual Review of Cell and Developmental Biology*, (13):83–117.
- Dogterom, M., Kerssemakers, J., Romet-Lemonne, G., and Janson, M. (2005). Force generation by dynamic microtubules. *Current opinion in Cell Biology*, (17):67–74.
- Efron, B. and Tibshirani, R. J. (1993). *An Introduction to the Bootstrap*. Chapman & Hall, New York.
- Fisher, N., Lewis, T., and Embleton, B. (1987). *Statistical Analysis of Spherical Data*. Cambridge Univ. Press, New York.
- Forgacs, G. and Newman, S. (2005). *Biological Physics of the Developing Embryo*. Cambridge Univ. Press, Cambridge.
- Gachet, Y., Tournier, S., Millar, J., and Hyams, J. (2004). Mechanism controlling perpendicular alignment of the spindle to the axis of cell division in fission yeast. *EMBO Journal*, (23):1289–1300.
- Gardner, R. (2003). The case for pre patterning in the mouse. *Birth defects research (part C)*, (75):142–150.
- Gilbert, S. (2006). *Developmental Biology*. Sinauer Associates Inc., Sunderland, 8th edition.

- Gittes, F., Meyhöfer, E., Baek, S., and Howard, J. (1996). Directional Loading of the Kinesin Motor Molecule as it Buckles a Microtubule. *Biophysical Journal*, 70:418–429.
- Gonczy, P. (2002). Mechanisms of spindle positioning: focus on flies and worms. *Trends in cell biology*, (12):332–339.
- Grill, S., Howard, J., Schaffer, E., Stelzer, E., and Hyman, A. (2003). The distribution of active force generators controls mitotic spindle position. *Science*, (301):518–521.
- Hamaguchi, M. and Hiramoto, Y. (2008). Analysis of the Role of Astral Rays in Pronuclear Migration in Sand Dollar Eggs by the Colcemid-UV Method. *Development, Growth & Differentiation*, 28:143–156.
- Hiiragi, T. and Solter, D. (2004). First cleavage plane of the mouse is not predetermined but defined by the topology of the two apposing pronuclei. *Nature*, 430(15):360–364.
- Karsenti, E., Nédélec, F., and Surrey, T. (2006). Modelling microtubule patterns. *Nature cell biology*, (11):1204–1211.
- Kimura, A. and Onami, S. (2005). Computer Simulations and Image Processing Reveal Length-Dependent Pulling Force as the Primary Mechanism for Male Pronuclear Migration. *Developmental Cell*, 8(5):765–775.
- Mallik, R. and Gross, S. (2004). Molecular motors: strategies to get along. *Current Biology*, (14):R971–R982.
- Manly, B. F. (1997). *Randomization, Bootstrap and Monte Carlo Methods in Biology*. Chapman & Hall, Boca Raton, Florida, 2nd edition.
- Mardia, K. and Jupp, P. (1987). *Directional Statistics*. John Wiley & Sons, West Sussex.
- Moré, J. (1977). The levenberg-marquardt algorithm: Implementation and theory. *Numerical Analysis, Lecture Notes in Mathematics*, (630):105–116.
- Motosugi, N., Bauer, T., Polanski, Z., Solter, D., and Hiiragi, T. (2005). Polarity of the mouse embryo is established at blastocyst and is not prepatterned. *Genes & Development*, (19):1081–1092.
- Nédélec, F. (2002). Computer simulations reveal motor properties generating stable antiparallel microtubule interactions. *Journal of Cell Biology*, (6):1005–1015.

- O'Connell, C. and Wang, Y. (2000). Mammalian spindle orientation and position respond to changes in a dynein dependent fashion. *Molecular Biology of the Cell*, (11):1765–1774.
- Page, E. (1954). Continuous Inspection Scheme. *Biometrika*, (41):100–115.
- Payne, C., Rawe, V., Ramalho-Santos, J., Simerly, C., and Schatten, G. (2003). Preferentially localized dynein and perinuclear dynactin associate with nuclear pore complex proteins to mediate genomic union during mammalian fertilization. *Journal of Cell Science*, (116):4727–4738.
- Plusa, B., Hadjantonakis, A., Gray, D., Piotrowska-Nitsche, K., Jedrusik, A., Papaioannou, V., Glover, D., and Zernicka-Goetz, M. (2005). The first cleavage of the mouse zygote predicts the blastocyst axis. *Nature*, 434(17):391–395.
- Purcell, E. (1977). Life at Low Reynolds Number. *American Journal of Physics*, (45):3–11.
- Tapani, S., Udagawa, J., Plusa, B., Zernicka-Goetz, M., and Lundh, T. (2009). Three dimensional mathematical modelling of pronuclei dynamics for the mouse. *Proceedings of the 10th European Congress of Image Analysis and Stereology*.
- Taylor, W. A. (2000). Change-Point Analysis: A Powerful New Tool For Detecting Changes. WEB:
<http://www.variation.com/cpa/tech/changepoint.html>, 20090929.
- Tsou, M., Ku, W., Hayashi, A., and Rose, L. (2003). PAR-dependent and geometry-dependent mechanisms of spindle positioning. *Journal of Cell Biology*, (160):5717–5730.
- Vallee, R. and Stehman, S. (2005). How dynein helps the cell find its center: a servomechanical model. *Trends in Cell Biology*, (15):288–294.
- Wolpert, L., Beddington, R., Brockes, J., Jessell, T., Lawrence, P., and Meyerowitz, E. (1998). *Principles of Development*. Oxford Univ. Press, New York, 1st edition.
- Zernicka-Goetz, M. (2005). Cleavage pattern and emerging asymmetry of the mouse embryo. *Molecular cell biology*, 6:919–928.
- Zernicka-Goetz, M. (2006). The first cell-fate decisions in the mouse embryo: destiny is a matter of both chance and choice. *Current opinion in Genetics & Development*, (16):406–412.

Contributed paper, Stereology and Image Analysis. Ecs10 - Proceedings of the 10th European Congress of ISS, (V.Capasso et al. Eds.), The MIRIAM Project Series, ESCULAPIO Pub. Co., Bologna, Italy, 2009.

Three dimensional mathematical modelling of pronuclei migration for the mouse

Authors: Sofia Tapani, Jun Udagawa, Berenika Plusa, Magdalena Zernicka-Goetz and Torbjörn Lundh

THREE DIMENSIONAL MATHEMATICAL MODELLING OF PRONUCLEI MIGRATION FOR THE MOUSE

SOFIA TAPANI¹, JUN UDAGAWA², BERENIKA PLUSA³, MAGDALENA ZERNICKA-GOETZ³
AND TORBJÖRN LUNDH¹

¹Mathematical Sciences, Chalmers and University of Gothenburg, SE-412 96 Göteborg, Sweden, ²Department of Developmental Biology, Shimane University, Izumo 693-8501, Japan, ³Wellcome Trust/Cancer Research UK Gurdon Institute, University of Cambridge, Tennis Court Road, Cambridge, CB2 1QR, UK
e-mail: sofia.tapani@chalmers.se

ABSTRACT

It is still an open question when the orientation of the embryonic-abembryonic axis of the mouse embryo is laid down. The two most explicit symmetry breaking events for the egg are the extrusion of the second polar body and the sperm entry. The main question addressed in this paper is what happens between the sperm entering the egg and fusion of the two pronuclei. Orientation of the apposing pronuclei probably plays a decisive role in the polarity of the developing embryo. In order to shed some lights on this intriguing question, a mathematical model that describes the pronuclei dynamics have been constructed in the form of a stochastic differential equation. The model concerns pronuclei migration from the time of the sperm entry to the fusion and spatial orientation of this fusion. The methodology consists of using stacks of confocal microscopy time-lapse images of the pronuclei migration together with statistical methods to identify realistic parameters in the model. Given different angles between the sperm entry and the position of the second polar body, the final model is then used to produce distributions of orientations of the meeting positions between the pronuclei. However, the main result is the suggested model itself which describes the main features of the migration. The fitted model is based on two forces of attraction. Migration is directed towards the centre but also towards the other pronucleus. Parameter values corresponding to the size of these forces are estimated from data of both eggs treated with a microtubule inhibitor and untreated eggs. Simulations from the model with the different model parameters are accomplished and distributions of meeting positions are plotted. These simulated distributions could for instance be used as initial value distributions for future models of egg cleavage.

Keywords: Confocal Microscopy, Developmental Biology, Image Analysis, Mathematical Modelling, Migration, Pronucleus.

INTRODUCTION

Developmental biology is the biology of the first events the living species experience. As the microscopical techniques improves and the amount of data increases the need for better and more effective analysis methods is developing. In this area there is a great interest towards a higher usage of methods from biophysics and biomathematics. Mathematical modelling of the microtubule dynamics in the *C. elegans* egg are used in for instance (Kimura and Onami, 2005), (Dogterom *et al.*, 2005) and many others.

The work of this paper has its background in the research of the Magdalena Zernicka-Goetz group at the Gurdon Institute in Cambridge. The group studies development of spatial patterning and determination of cell fate of the early mouse embryo.

As most mammalian eggs, the mouse egg is a highly regulative system. In being so, it is still an open question of when cell fates are fixed, (Davies and Gardner, 2002), (Davies and Gardner,

2003), (Gardner, 2003), (Hiragi and Solter, 2004), (Motosugi *et al.*, 2005), (Plusa *et al.*, 2005), (Zernicka-Goetz, 2005), (Zernicka-Goetz, 2006). There exists different viewpoints of definitions of total randomness and pattern bias against rigidity and determinative behaviour. However, our aim is to show that these two possible explanations do not exclude each other but can both simultaneously affect the cell fates. Cells may have a pattern, or a set of rules, to follow and at the same time be influenced of the stochasticity of the chemical system and the cytoplasmic environment inside the egg.

At this time it remains unanswered how the embryonic-abembryonic axis of the mouse blastocyst is first established. Cell-fate is flexible meaning that the development can recover from perturbations (Gilbert, 2006). Previous results indicate that the first cleavage is preferably occurring along the short axis of the egg (Zernicka-Goetz, 2005). The short axis is in turn related to sperm entry and migration of the pronuclei. The second polar body and the sperm entry point could together make up a coordinate system for the axis formation of the later embryo. Other

studies of the mouse development show deviating results of when patterning is initiated in the egg. For instance (Davies and Gardner, 2002) and (Hiiragi and Solter, 2004). Some of these studies that conclude that the pattern formation starts later in the embryo have been conducted in 2D. However, the authors of this paper think it is important to consider this as a 3D problem since ignoring one of the three dimensions may introduce some bias.

One purpose of having a model for the migration is to be able to more easily visualize the fertilization process to answer these questions. A model of this kind could be used to predict outcomes from for instance the point of sperm entry by simulating different scenarios. It could provide initial conditions to further models of cell division and differentiation. Moreover, values of model parameters can be used to quantify treatment or measurement effects on the egg.

We are using inspiration from developmental biology literature and potential theory to produce a model for the migration. In setting up the model, data from confocal time-lapse DIC images of mouse eggs have been used to record the 3D-coordinates of the pronuclei up until the first division of the egg.

MATERIALS AND METHODS

Confocal microscopy DIC time-lapse images of mouse eggs were used as data input for the migration model. The imaging method is described more thoroughly in Plusa *et al.* (2005). Recordings of the pronuclei positions have been carried out, for all three dimensions. The measuring procedure is performed, until the first division, positions are expressed as (m_x, m_y, m_z) for the male pronucleus and (f_x, f_y, f_z) respectively for the female. Some of the time points have errors in them, e.g. missing slices or inconclusive images, so that they must be discarded. Hence the time points used are not always evenly spaced.

Each sequential image consists of seven z-scans with $14\ \mu\text{m}$ distance apart. A mouse egg has a diameter of about $80 - 100\ \mu\text{m}$. The width and height of each pixel correspond to $0.37\ \mu\text{m}$. This gives an uncertainty which is quite large in coordinates perpendicular to the image planes (z-axis) compared to the image plane coordinates (x- and y-axes). Sequential images are taken with 5 minutes intervals. Figure 1 is an example of a single time-lapse image at the third z-scan level of one egg. Both the female and the male pronuclei are visible as fairly circular structures in the egg.

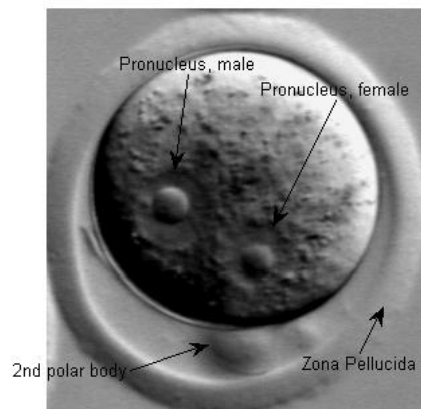


Fig. 1. An example of a time-lapse image of a mouse egg. The pronuclei are visible, the female pronucleus to the right and male to the left in the image respectively.

It is the artificial coordinate system introduced by the imaging technique of confocal microscopy that is used for the analysis. The first two coordinates are set by the image plane and the third is set by the z-stack. One purpose of having this non-natural coordinate system is to keep control over the low resolution in the z-axis. Strange values or results for this coordinate could then be related back to this property. At this stage of the modelling the egg is assumed to be spatially homogeneous for simplicity. How this relates to the actual environment of the pronuclei, may be questioned. Cytoplasm can be denser in some directions if the egg is flattened. For instance, during sperm entry the egg is believed to have an oval rather than a circular shape (Zernicka-Goetz, 2005). Also the cytoplasm and the cytoskeleton undergo quite large changes during the fertilization. These processes could lead to lesser or larger crowding in the surrounding cytoskeleton of the pronuclei. In this paper, modelling is conducted on a macroscopic level, meaning that we will address the pronuclei mechanics and not the cytoplasm directly. Hence no molecular reactions have been modelled either. The assumptions of homogeneity leads to the same kind of behaviour in all directions of the egg.

Manual observations of the migration indicate that not only do the pronuclei move towards the centre of the egg but also toward each other. For example, the experiments by Hamaguchi and Hiramoto (2008) show this kind of behaviour of sand dollar eggs. Therefore in our model below the pronuclear migration is assumed to depend on two forces of attraction, F_C and F_A . This could be seen as simple representations of a more complex force compound. Where F_C represents attraction towards the centre and F_A represents

attraction towards the other pronucleus. See also Figure 2. Note that the size of the force F_A is equal of strength for both pronuclei but oppositely directed.

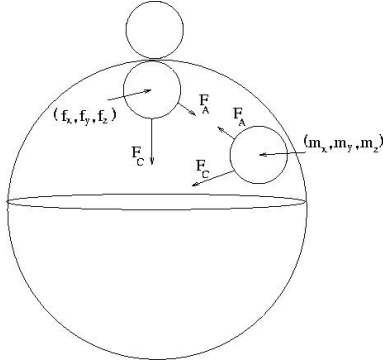


Fig. 2. Schematic picture of the two attraction forces. The positions of the pronuclei are recorded with three coordinates regarding the position in the image plane (x - and y -coordinates) and estimated height (z -coordinate) in the z -stack.

When the male and the female pronucleus move toward the centre and to each other, the migration depends on microtubule guiding the movements. The microtubule are bipolar structures which are involved in many cellular processes such as mitosis and cytokinesis, (Gilbert, 2006), (Wolpert *et al.*, 1998). They are guided from the centrosomes provided by the sperm and the female pronucleus. Along the microtubule, motor proteins can move towards both the plus end and the minus end of the microtubule (kinein and dynein). The intracellular medium is a very crowded environment and pronuclei migration is basically movement at low Reynolds numbers, see for instance (Purcell, 1977) and (Forgacs and Newman, 2005). A world of this kind leads to a model with only frictional forces and no inertia. Frictional forces are mainly due to the surrounding cytoplasm and cytoskeleton. If only frictional forces are present, the forces should be proportional to the velocity of the pronucleus. The total force compound acting on a pronucleus will then be $F_A + F_C$.

First we give a model for F_C , which represents the centring part of the forces acting on the pronucleus. The special structure of the microtubule will give rise to both pulling and pushing forces. It might be difficult to see which one to choose in a simple model like ours. Very few, if any, results can be found for mammalian species. Kimura and Onami (2005) however write about the length-dependent pulling force as primary mechanism for the *C. elegans* male pronuclear migration. This primary mechanism has been modelled such as having longer microtubule leads to a more powerful force. Microtubules that grow towards the cortex of the egg have a limited length,

which leads to that the microtubules directed along the centre of the egg are the longest and also give a stronger pulling force. The pronuclei would migrate towards the centre. The idea is to have a force that is based on friction and does not blow up at the centre or at the boundary of the egg, when pronuclei are moving against the drag from the cytoplasm. Note that the modelling is conducted in 3D, and \mathbf{m} and \mathbf{f} are 3D locations of the male and female pronucleus respectively. We make the following ansatz for the centring part

$$\frac{d\mathbf{f}}{dt} = C \frac{-\mathbf{f}}{(R - |\mathbf{f}| + \varepsilon)|\mathbf{f}|}, \quad (1)$$

for the female pronucleus, and analogously for the male pronucleus. Here R is the radius of the egg and C , ε constants that have to be estimated. The model in (1) gives a velocity for the pronucleus which flattens out at the centre of the egg. Close to the centre this force will be smaller and close to the boundary of the egg it will be larger. The parameter ε assures that the velocity is not too large right at the boundary of the egg. Equation (1) builds on the assumption that the pronuclei move with the same speed to the centre of the egg and hence have the same constant C .

Next, we model F_A , the attraction of the pronuclei toward each other. This force is modelled by finding inspiration in the theory of electrostatics and charged particles, which is reasonable given the bipolarity of the microtubule. It is desirable that the attraction increases with decreasing distance between the pronuclei. We make the following addition to the earlier ansatz of Equation (1)

$$\frac{d\mathbf{f}}{dt} = C \frac{-\mathbf{f}}{(R - |\mathbf{f}| + \varepsilon)|\mathbf{f}|} + A \frac{\mathbf{m} - \mathbf{f}}{(|\mathbf{m} - \mathbf{f}|^{\alpha+1} + \gamma)}, \quad (2)$$

for the female pronucleus. The additional term to the differential equation for the male dynamics is almost equivalent but added with opposite sign. The constant γ is added for gaining a more feasible model for the pronuclei dynamics. We will here give a motivation for Equation (2) with $\alpha = 2$. In (Payne *et al.*, 2003) it is suggested that higher density of microtubule connected to the other pronucleus yields a higher force. Given that the distance between the approaching pronuclei is ρ , and the radius of a pronucleus is r , we get from similarity that $\frac{r}{h} \approx \frac{\rho}{r}$, see Figure 3. Here h is the height of the intersecting microtubule area of one pronucleus. This area is then proportional to the quantity $\frac{r^4}{\rho^2}$, hence the resulting force is proportional to one over the squared distance between the pronuclei. The force of attraction is modelled to depend on how big the connecting "microtubule surface" is. If more

microtubules are connected it should yield a larger force. This is the first basic assumption we make.

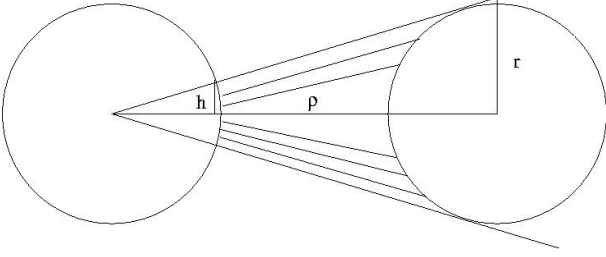


Fig. 3. Illustration of how the attraction between the pronuclei is modelled. The attractive force is modelled to depend on the connected area of microtubules sent out. Similarity yields a force proportional to $1/\rho^2$, where ρ is the distance between the pronuclei.

The environment in the mouse egg is not simple fluid material. It is on the contrary quite complex and the microtubule guided migration is not fulfilled without resistance from the surrounding cytoplasm. This leads to a natural variation in the data which needs to be taken into account for into the model. This random variation is modelled as Brownian motion as

$$\begin{aligned} d\mathbf{B}(t) &= \mathbf{B}(t+dt) - \mathbf{B}(t) = \\ &= (B_x(t+dt) - B_x(t), B_y(t+dt) - B_y(t), \\ &\quad B_z(t+dt) - B_z(t)), \end{aligned} \quad (3)$$

where $B_i(t) \sim N(0, \sigma^2)$. Here we have assumed that the egg is spatially homogenous. This makes it easier to estimate the variation of the noise since then the variation is assumed to be equal for all axes. The noise is added to Equation (2) yielding the following complete stochastic differential equation model for the dynamics of the female pronucleus

$$\frac{d\mathbf{f}}{dt} = C \frac{-\mathbf{f}}{(R - |\mathbf{f}| + \varepsilon)|\mathbf{f}|} + A \frac{\mathbf{m} - \mathbf{f}}{(|\mathbf{m} - \mathbf{f}|^{\alpha+1} + \gamma)} + d\mathbf{B}(t), \quad (4)$$

RESULTS

The model parameters C , A , ε , γ and α are estimated by a nonlinear least squares method. It is the Line-Search type algorithm that is used in the optimization. The best fit is given by $\varepsilon = 0$, $\gamma = 0$, $C = 0.05R$, $A = 0.09R$ and $\alpha = 1.81$. Where, R is the radius of the egg. Note that the value of α is not far from the assumed value of 2. The standard deviation of the noise is estimated to $\sigma = 0.02R$. It should be

noted that despite the limited data the values of the parameters are quite reasonable. Parameter estimation leads to the following final version of the model.

$$\frac{d\mathbf{m}}{dt} = C \frac{-\mathbf{m}}{(R - |\mathbf{m}|)|\mathbf{m}|} + A \frac{\mathbf{f} - \mathbf{m}}{|\mathbf{m} - \mathbf{f}|^3} + d\mathbf{B}(t), \quad (5)$$

and analogously for the female pronucleus.

In order to visualize the consequences of the model for the migration and to see how well the model describes the data, simulations have been performed and the simulated pronuclei dynamics have been plotted. For one specific egg the starting coordinates have been used in one run of the simulation and the result is shown in Figure 4. The actual trajectories recorded are plotted in Figure 5. It can be seen that at least this simulated trajectory looks like the one in the real data. The model succeeds to mimic some of the behaviour that is observed. However there seems to be a larger spread in the simulated data than in the real ones. This may be a feature of the analyzed eggs having quite large individual variation.

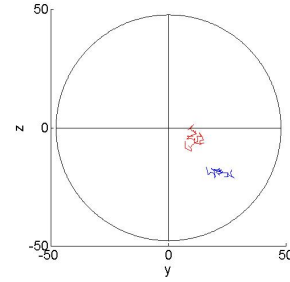


Fig. 4. Plot of simulated data from one run of the model in the yz -plane. The male trajectory is plotted with blue colour and the female with red respectively.

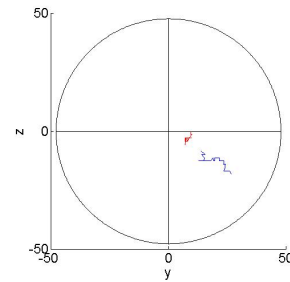


Fig. 5. Plot of manual data for egg 31 in the yz -plane. The male trajectory corresponds to blue colour and the female to red respectively.

Monte Carlo simulations of the dynamics are carried out ten thousand times to produce a distribution of trajectories for the pronuclei. At each simulation the meeting position is recorded, or rather the angles that specify the vector between the centre points of the approaching pronuclei. Simulations of this kind could

in turn provide initial conditions for future models regarding cleavage of the egg. It could be interesting to see what kind of distributions of meeting positions different sperm entry points would lead to.

The two dimensional distribution for both the azimuthal (θ , the angle around the equator of the egg) and elevational (ϕ) angle of the vector between the pronuclei is recorded. See Figure 6, where this have been plotted for a sperm entry of 45° from the second polar body. The polar body is always at the north pole and the sperm entry point (SEP) is varied in the elevational angle but held at azimuthal angle 0° . Meeting planes are concentrated in the upper hemisphere of the egg, hence positive latitudinal angles. Note that azimuthal angle of 180° , is equal to azimuthal angle of -180° . Red colour means high counts and blue lower.

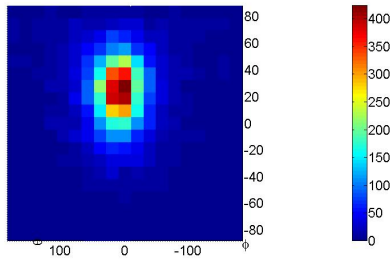


Fig. 6. Simulation of pronuclei meetings, yielding a distribution of the azimuthal and elevational angle of the vector between the pronuclei centers. Sperm entry is at an elevational angle of 45° .

According to this model a sperm entry further from the second polar body would introduce a wider spread of where the pronuclei meet and possibly also a wider spread of the cleavage plane. The main weight in the angular distributions seems to be positioned at the same place for the different sperm entry points.

We also have data available from two eggs treated with Cytochalasin B (CB). CB is known for being an inhibitor of microtubule growth. This substance is sometimes used for slowing down the migration to be able to gain images of improved quality. We have examined what the consequences of the CB treatment are for the model parameters. What is more important than the actual results for our model is the possibility of using parameter estimates from data of diverging characteristics in simulations. Results from these estimations could in turn be used for testing if techniques or treatments used are too invasive.

The parameters for the pronuclear migration are reestimated for the CB data with the same method as before. The centring constant is $C = 0$ and the attraction constant is $A = 0.02R$. γ is estimated to zero again. Furthermore $\alpha = 1.99$ and $\sigma = 0.005R$, and R

is, as before, the radius of the egg. Since CB hinders the microtubule to grow, the rate of migration would be expected to decrease. This can be seen in the values of the parameter estimates as lower force constants. The centring force seems actually to have vanished.

Simulations of meeting positions have also been done with the parameter values estimated from the CB data. The results are shown in Figure 7. At a first glance, the distributions in Figures 6 and 7 seem similar. However, looking closely it can be seen that the spread is lower in the distribution for the eggs treated with CB. According to the simulations we get that a lower centring force gives a smaller spread in the positions where pronuclei meet. If these positions are important in the future cleavage of the egg this may be an indication of an undesired invasiveness of the treatment.

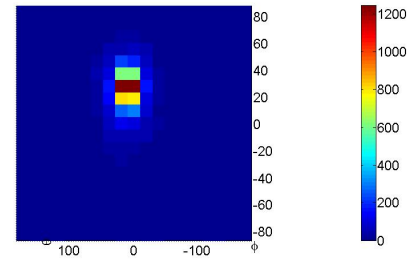


Fig. 7. Simulated distributions of meeting angles for the data treated with Cytochalasin B. Compare with Figure 6. Since the centering constant is set to zero a lower spread of the distribution is achieved.

DISCUSSION

We have introduced a model for the pronuclei migration in the mouse egg and described how it can be applied to actual data of fertilized mouse eggs. The model is a first attempt to describe such processes at a mechanical level. The model is based on a few simple assumptions and is meant to serve as the starting point for a more complex and biologically more relevant model. The model was even reduced further given the data, to Equation (5). In spite of being simple, the model still gives some nice results and an idea of what could be done and tested. Our results indicate that the CB treatment affects the pronuclei migration, which is something we would like to investigate further.

However there are a lot of issues to address before going further. As we have already mentioned, the data available is quite limited. In order to increase the accuracy of the estimation, one would need a variety of eggs with pronuclei starting in uniformly distributed distances from each other. As the imaging

technique continuously improves it is possible to have a better resolution in both the image plane data and a smaller distance between the z-scan levels. Fertilization dynamics differ quite largely from egg to egg but z-scan resolution is still the biggest limitation of the data. However, one should not push this too far. It is important not to use imaging techniques that affect the migration in a not desired way as the egg is a sensitive system.

Our main aim is to obtain a model that is more consistent with the developmental biological literature than our current model is. It may be preferable to start with modelling the cytoskeleton in a more thorough way, since this is what the microtubule actually clings to when they are engaged in the pronuclear migration. Our intention is to make use of better analysis methods such as semiautomatic or automatic image analysis methods for tracking the pronuclei in the image sequences. It is desired to remove as many human errors as possible. Image analysis methods are not only useful for increasing objectivity but also for making it possible to analyze pronuclei trajectories more effectively. The manual measuring procedure is not an easy task but something that should be performed by an experienced person with good knowledge of the migration process.

Finally, it should be recognized that the model gives expected results for especially the eggs treated with the microtubule inhibitor. Also, we give a motivation for having a certain expression for the attraction between the pronuclei which is in turn specified by estimating the parameters from the data.

ACKNOWLEDGEMENTS

Thanks goes to associate professor Aila Särkkä at the Department of Mathematical Sciences division of Mathematical Statistics at Chalmers and the University of Gothenburg, for her invaluable comments and time.

REFERENCES

- Davies T, Gardner R (2002). The plane of first cleavage is not related to the distribution of sperm components in the mouse. *Human Reproduction* 17:2368–79.
- Davies T, Gardner R (2003). Philosophical transactions: Biological sciences. *Human Reproduction* 358:1331–9.
- Dogterom M, Kerssemakers J, Romet-Lemonne G, Janson M (2005). Force generation by dynamic microtubules. *Current opinion in Cell Biology* :67–74.
- Forgacs G, Newman S (2005). *Biological Physics of the Developing Embryo*. Cambridge: Cambridge Univ. Press.
- Gardner R (2003). The case for prepatterning in the mouse. *Birth defects research part C* :142–50.
- Gilbert S (2006). *Developmental Biology*. Sunderland: Sinauer Associates Inc., 8th ed.
- Hamaguchi M, Hiramoto Y (2008). Analysis of the role of astral rays in pronuclear migration in sand dollar eggs by the colcemid-uv method. *Development Growth Differentiation* 28:143–56.
- Hiiragi T, Solter D (2004). First cleavage plane of the mouse is not predetermined but defined by the topology of the two apposing pronuclei. *Nature* 430:360–4.
- Kimura A, Onami S (2005). Computer simulations and image processing reveal length-dependent pulling force as the primary mechanism for male pronuclear migration. *Developmental Cell* 8:765–75.
- Motosugi N, Bauer T, Polanski Z, Solter D, Hiiragi T (2005). Polarity of the mouse embryo is established at blastocyst and is not prepatterned. *Genes Development* :1081–92.
- Payne C, Rawe V, Ramalho-Santos J, Simerly C, Schatten G (2003). Preferentially localized dynein and perinuclear dynactin associate with nuclear pore complex proteins to mediate genomic union during mammalian fertilization. *Journal of Cell Science* :4727–38.
- Plusa B, Hadjantonakis A, Gray D, Piotrowska-Nitsche K, Jedrusik A, Papaioannou V, Glover D, Zernicka-Goetz M (2005). The first cleavage of the mouse zygote predicts the blastocyst axis. *Nature* 434:391–5.
- Purcell E (1977). Life at low Reynolds number. *American Journal of Physics* :3–11.
- Wolpert L, Beddington R, Brockes J, Jessell T, Lawrence P, Meyerowitz E (1998). *Principles of Development*. New York: Oxford Univ. Press, 1st ed.
- Zernicka-Goetz M (2005). Cleavage pattern and emerging asymmetry of the mouse embryo. *Molecular cell biology* 6:919–28.
- Zernicka-Goetz M (2006). The first cell-fate decisions in the mouse embryo: destiny is a matter of both chance and choice. *Current opinion in Genetics Development* :406–12.